European Journal of Medicinal Chemistry 100 (2015) 197–209

Contents lists available at ScienceDirect

European Journal of Medicinal Chemistry

journal homepage: http://www.elsevier.com/locate/ejmech

Research paper

Synthesis and evaluation of thymidine kinase 1-targeting carboranyl pyrimidine nucleoside analogs for boron neutron capture therapy of cancer

Hitesh K. Agarwal [a, 1, 2], Ahmed Khalil [a, 1, 3, 4], Keisuke Ishita [a], Weilian Yang [b, 5], Robin J. Nakkula [b, 6], Lai-Chu Wu [c], Tehane Ali [a], Rohit Tiwari [a, 7], Youngjoo Byun [d], Rolf F. Barth [b], Werner Tjarks [a, *]

[a] Division of Medicinal Chemistry & Pharmacognosy, The Ohio State University, Columbus, OH, USA
[b] Department of Pathology, The Ohio State University, Columbus, OH, USA
[c] Department of Internal Medicine, The Ohio State University, Columbus, OH, USA
[d] College of Pharmacy, Korea University, Sejong, Republic of Korea

ARTICLE INFO

Article history:
Received 20 January 2015
Received in revised form
24 May 2015
Accepted 26 May 2015
Available online 27 May 2015

Keywords:
Carboranyl pyrimidine nucleoside analog
Thymidine kinase 1 (TK1)
Carborane
Boron neutron capture therapy (BNCT)

ABSTRACT

A library of sixteen 2nd generation amino- and amido-substituted carboranyl pyrimidine nucleoside analogs, designed as substrates and inhibitors of thymidine kinase 1 (TK1) for potential use in boron neutron capture therapy (BNCT) of cancer, was synthesized and evaluated in enzyme kinetic-, enzyme inhibition-, metabolomic-, and biodistribution studies. One of these 2nd generation carboranyl pyrimidine nucleoside analogs (**YB18A** [**3**]), having an amino group directly attached to a *meta*-carborane cage tethered *via* ethylene spacer to the 3-position of thymidine, was approximately 3–4 times superior as a substrate and inhibitor of hTK1 than **N5-2OH (2**), a 1st generation carboranyl pyrimidine nucleoside analog. Both **2** and **3** appeared to be 5′-monophosphorylated in TK1(+) RG2 cells, both *in vitro* and *in vivo*. Biodistribution studies in rats bearing intracerebral RG2 glioma resulted in selective tumor uptake of **3** with an intratumoral concentration that was approximately 4 times higher than that of **2**. The obtained results significantly advance the understanding of the binding interactions between TK1 and carboranyl pyrimidine nucleoside analogs and will profoundly impact future design strategies for these agents.

Abbreviations: 3CTAs, 3-carboranyl thymidine analogs; ^{10}B, boron-10; ATCC, American type culture collection; AZT, zidovudine; B, boron; BNCT, boron neutron capture therapy; *Ba*TK, *Bacillus anthracis* thymidine kinase; DEAE, diethylaminoethanol; DMEM, Dulbecco's modified eagle's medium; dThd, thymidine; d4T, stavudine; ESI+ or ESI−, electrospray ionization positive or negative ion mode, respectively; FBS, fetal bovine serum; HRP, horseradish peroxidase; hTK1, human thymidine kinase 1; ICP-OES, inductively coupled plasma-optical emission spectroscopy; IACUC, institutional animal care and use committee; LET, linear energy transfer; MP, monophosphate; PEI, polyethylenimine; PTA, phosphate transfer assay; RP-18, reversed-phase 18; rPR, relative phosphorylation rate; *Sa*TK, *Staphylococcus aureus* thymidine kinase; siRNA, small interfering ribonucleic acid; SM, supplementary materials; TBDMS, *tert*-butyldimethylsilyl; TK1, thymidine kinase 1.

* Corresponding author. Division of Medicinal Chemistry & Pharmacognosy, The Ohio State University, 500 West 12th Avenue, Columbus, OH 43210, United States.
E-mail address: tjarks.1@osu.edu (W. Tjarks).

[1] H.K.A. and A.K. contributed equally to the paper.
[2] Current address: Department of Neuroscience, Mount Sinai School of Medicine, New York, NY, USA.
[3] Current address: Laboratory of Biochemical Pharmacology, Emory University, Atlanta, GA, USA.
[4] Permanent address: Chemistry Department, Faculty of Science, Zagazig University, Zagazig, Egypt.
[5] Current address: Changzhou, China.
[6] Current address: School of Environmental and Natural Resources, College of Food, Agriculture and Environmental Science, The Ohio State University, Columbus, OH, USA.
[7] Current address: Department of Chemistry and Biochemistry, University of Notre Dame, Notre Dame, IN, USA.

http://dx.doi.org/10.1016/j.ejmech.2015.05.042
0223-5234/

1. Introduction

TK1-like enzymes, including human thymidine kinase 1 (hTK1), *Bacillus anthracis* TK (*Ba*TK), and *Staphylococcus aureus* TK (*Sa*TK), play essential roles in the biosynthetic salvage pathways of nucleotide synthesis, complementing the *de novo* pathways particularly in proliferating cells and bacteria [1–6]. In normal human cells, TK1 activity is high only in S-phase. In cancer cells, however, TK1 activity can remain also high in other phases of the cell cycle [7–9].

Clinically relevant agents that rely on TK1 activity include the HIV/AIDS prodrugs zidovudine (AZT) and stavudine (d4T) [10]. Both compounds are analogs of the endogenous TK1 substrate, thymidine (dThd, **1**, Fig. 1). They are effectively 5′-monophosphorylated by TK1. Their ultimate mechanism of action, however, is based on the subsequent formation of a cytotoxic triphosphate metabolite by other kinases. Other biomedically relevant analogs of **1** that possibly rely on 5'-monophosphorylation by TK1 are 3-carboranyl thymidine analogs (3CTAs). The agents were developed as boron delivery agents for boron neutron capture therapy (BNCT) of brain tumors [11,12]. Other types of carboranyl nucleoside derivatives were developed for the same and other purposes [13–17]. BNCT is a binary cancer treatment system that relies on the accumulation of boron-10 (^{10}B) in tumor cells followed by external neutron irradiation. Subsequent capture of neutrons by ^{10}B results predominantly in high linear energy transfer (LET) ionizing radiation, i.e., $^{4}He^{2+}$ (α-particle) and $^{7}Li^{3+}$ nuclei. These particles can selectively destroy tumor cells because of their limited path lengths of <10 μm in biological tissue. Prerequisite for the success of BNCT is the selective accumulation of ^{10}B in tumor vs. normal cells [18,19].

First generation 3CTAs, such as **N5-2OH (2**, Fig. 1), were found to be good substrates of TK1, despite having a bulky and highly lipophilic carboranyl substituent [20] tethered *via* alkyl spacer to the 3-position. Preferential uptake of **2** by TK1(+) vs. TK1(−) cells *in vitro*, presumably involving intracellular trapping of its 5′-monophosphate, was observed [21,22]. Consequently, a favorable *in vivo* biodistribution profile of **2** in tumor bearing rodents, possibly encompassing tumor-selective accumulation by intracellular accumulation of the 5′-monophosphate metabolite, led to promising preclinical BNCT of rats with brain tumors [21,22]. However, the need for improvement of 1st generation 3CTAs became apparent during these studies. They had moderate capacity to inhibit TK1 activity, i.e., to compete with endogenous **1** for phosphorylation at the substrate-binding site [11,23].

In order to make further progress in achieving the crucial objective of improved TK1 substrate and inhibitory capacities, the design, synthesis, and biological evaluation of carboranyl pyrimidine nucleoside analogs with amino- or amido functionalities in *meta* (1,7)-carborane cluster-containing side chains either at the 3- or 4-position will be described in this paper (see Fig. 1 for the atom numbering of pyrimidine nucleosides).

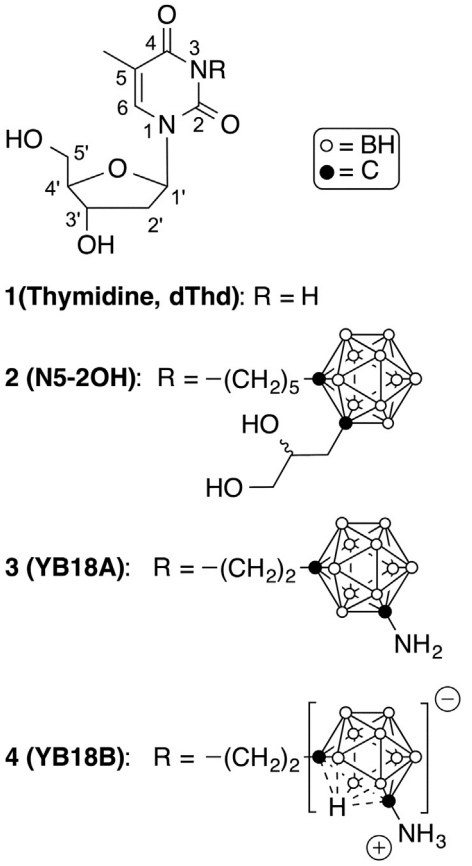

Fig. 1. Structures of **1**, the first generation 3CTA **2**, and the second generation 3CTAs **3** and **4**.

2. Results

2.1. Design and chemistry

All TK1-like enzymes have similar overall 3-D fold including the presence of a structural component that has been designated as the 'lasso-loop' [6,24]. The enzymes undergo significant conformational changes upon binding of **1** and ATP [25,26]. In the apo state, the lasso loop is folded away from the substrate-binding site whereas in the holo state, the lasso loop covers the substrate-binding site tightly by forming hydrogen bonds with **1**, primarily *via* main chain atoms.

Preliminary computational docking of 1st generation 3CTAs, such as **2**, to TK1 crystal structures led to the hypothesis that initial substrate binding results in incomplete closure of the lasso loop, leaving the bulky carborane cage outside of the active site, and that some hydrogen bonds are lost because of the 3-substitution [23,27,28]. This model may explain the moderate TK1 inhibitor characteristics of 1st generation 3CTAs because endogenous **1** may still have ample competitive access to the substrate binding site. It is also conceivable that a location of the highly hydrophobic carborane cage outside of the enzyme is disrupting the hydrogen bond network of water molecules and that this is contributing to the lack of binding of 3CTAs to TK1. It needs to be emphasized, however, that the exact molecular interactions between 3CTAs and TK1 amino acid residues remain unknown.

Based on the current hypothesis on 3CTA-TK1 interactions, previous efforts in our laboratories have focused on the introduction of hydrogen bond donor/acceptors, including hydroxyl-, amidino-, and guanidino groups, in a spacer element between the carborane cluster and the scaffold of **1** in 2nd generation 3CTAs to re-establish hydrogen bonds between substrate and enzyme that were lost due to the 3-substitution [29,30]. These groups were mostly placed in close proximity to the 3-position. Unfortunately, these 3CTAs did not prove to be superior to **2** as TK1 substrates and inhibitors. In the case of some compounds, lack of stability was another problem [29]. The design concept for carboranyl pyrimidine nucleosides discussed in this paper explores the introduction of hydrogen bond donor/acceptor amino- or amido groups in spacer elements between *meta*-carborane cluster and pyrimidine nucleoside scaffold, both at the 3-(Schemes 1–3) and the 4-(Scheme 4) position. In addition, **3** (**YB18A**) and **4** (**YB18B**) (Fig. 1), both containing an amino group directly attached to a *meta*-carborane cluster tethered *via* ethylene spacer to the 3-position, were prepared for detailed enzyme kinetic and inhibition studies. The syntheses of both compounds and their

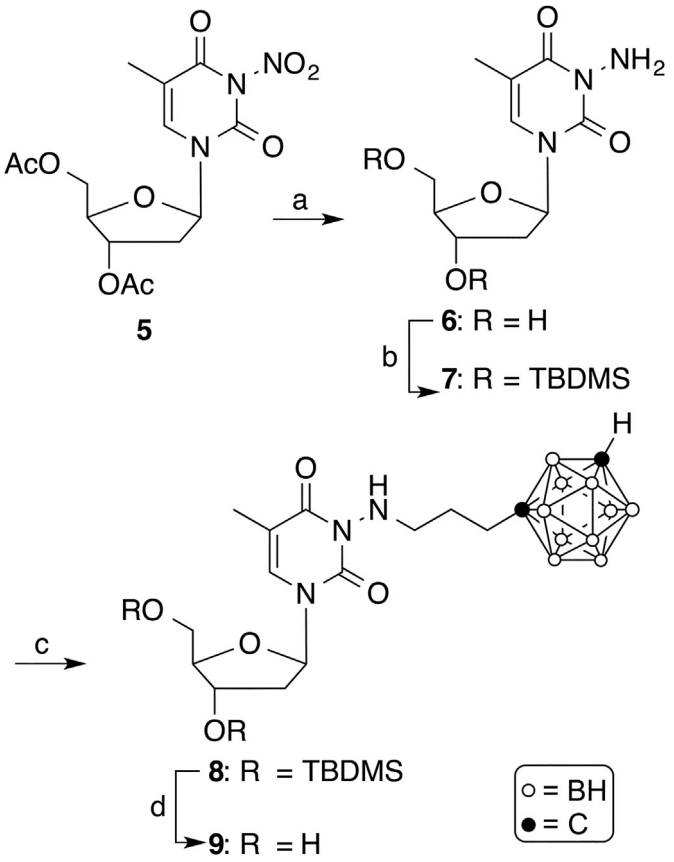

Scheme 1. Synthesis of compound **9**. Reagents and conditions: (a) $NH_2NH_2 \cdot H_2O$, 1M KOH in MeOH/H_2O (1/2), MeOH, 2 h, rt; (b) *tert*-butyldimethylsilyl chloride, imidazole, DMF, overnight, rt; (c) 1-(3-iodopropyl)-*closo*-1,7-carborane [35], NaH, DMF, 90 °C, 2 h; (d) TBAF, THF, 2 h, rt.

evaluation in preliminary phosphate transfer assays (PTAs) were described previously by us [31]. Compound **2**, synthesized according to a procedure described previously [32], and **1** were used in all biological studies as reference compounds.

The synthesis of the target compound **9** is shown in Scheme 1. Modifying a procedure previously described by Ariza et al. for the synthesis of ^{15}N-enriched 5′-*O*-acetyl-3-amino-2′-3′-isopropylidene uridine [33], 3′,5′-diacetyl-3-nitrothymidine [34] (**5**) was treated with hydrazine hydrate and potassium hydroxide in a mixture of MeOH and H_2O at room temperature for 2 h to yield 3-aminothymidine (**6**) in 28% yield following purification by reversed phase (RP)-18 HPLC using 0.1% TFA in H_2O as the solvent system followed by evaporation. According to ^{13}C NMR (SM), compound **6** did not retain trifluoroacetate. *tert*-Butyldimethylsilyl-(TBDMS) protection of the 3′- and 5′-hydroxyl groups of **6** was accomplished by stirring *tert*-butyldimethylsilyl chloride in the presence of imidazole in DMF at room temperature overnight to produce **7**, which was isolated in 90% yield following purification by silica gel column chromatography. Compound **7** was *N*-alkylated with 1-(3-iodopropyl)-*closo*-1,7-carborane [35] in the presence of sodium hydride in DMF at 90 °C for 2 h to produce compound **8** in 30% yield. The deprotection of the TBDMS-groups was accomplished by treatment with TBAF in THF at room temperature for 2 h to produce target compound **9** in 63% yield. Compounds **8** and **9** were purified by silica gel chromatography. In the synthesis of **9**, the *N*-alkylation at the hydrazine-type primary amine had to be performed using 3′,5′-TBDMS-protected **7** because the reaction did not proceed with its unprotected precursor **6**.

The synthesis of target compounds **16**–**22** is described in Scheme 2. 3-Cyanomethylthymidine (**10**) [29], 3-(2-cyanoethyl) thymidine (**11**), and 3-(3-cyanopropyl)thymidine (**12**) were synthesized by reacting **1** with the appropriate cyanoalkyl halide in the presence of potassium carbonate in DMF/acetone (1/1, v/v) at 60 °C for 8 h, as described previously by Agarwal et al.[29]. The compounds were purified by silica gel chromatography in 78–97% yield. Reduction of **10**–**12** using potassium borohydride and Raney nickel in EtOH at room temperature for 1 h [36] produced compounds **13**–**15** in 67–82% yield following purification by RP-18 HPLC (MeOH/H_2O solvents systems containing 0.1% TFA) followed by evaporation. Compounds **13**–**15** were 3-alkylated with 1-(2-iodoethyl)-*closo*-1,7-carborane [35], 1-(3-iodopropyl)-*closo*-1,7-carborane [35], and 1-(4-iodobutyl)-*closo*-1,7-carborane [35], respectively, in the presence of sodium hydride in DMF at 90 °C for 2 h to produce target compounds **16**–**22**. Despite the presence of free hydroxyl groups in **13**–**15**, alkylation predominantly resulted in the formation of N-monoalkylated and, to a lesser extent, N,N-dialkylated product. Compounds **16**–**22** were purified by RP-18 HPLC (MeOH/H_2O solvents systems containing 0.1 % TFA). Following evaporation, yields ranged from 4 to 12 % for compound **16**–**18** and 26–48% for **19**–**22**. The low yields found for **16**–**18** reflect a significant level of decomposition observed of these compounds especially during reactions and storage. According to ^{13}C NMR (SM), some of the compounds **13**–**22** retained traces of trifluoroacetate.

The synthesis of amido group containing target compounds **28**–**30** is shown in Scheme 3. The reaction of 3′,5′-bis-*O*-(*tert*-butyldimethylsilyl)thymidine [37] (**23**) with methyl bromoacetate in the presence of sodium hydride in anhydrous acetone at room temperature for 2 h gave compound **24** in 69% yield following purification by silica gel chromatography. The aminolysis of the ester in **24** was achieved by acyl transfer catalysis [38] using a mixture of 1,2,4-triazole and 1,8-diazabicyclo[5.4.0]undec-7-ene (DBU) and either 1-(2-aminoethyl)-*closo*-1,7-carborane [35], 1-(3-aminopropyl)-*closo*-1,7-carborane [35], or 1-(4-aminobutyl)-*closo*-1,7-carborane [35]. The reaction was carried at 80 °C for 3 days without solvent to produce compounds **25**–**27** in 12–48% yields. Aminolysis was carried out with 3′,5′-TBDMS-protected nucleoside in accordance with a previously reported procedure [39].

Deprotection of the TBDMS-groups of **25**–**27** was accomplished with TBAF in THF at room temperature for 2 h to produce target compounds **28**–**30** in 71–93% yields. Compounds **25**–**30** were purified by silica gel chromatography.

The synthesis of the N4-carboranylalkyl-5-methyl-2′-deoxycytidine analogs **35**–**37** is shown in Scheme 4. The reaction of compound **31** [39] with 1-(2-aminoethyl)-*closo*-1,7-carborane [35], 1-(3-aminopropyl)-*closo*-1,7-carborane [35], or 1-(4-aminobutyl)-*closo*-1,7-carborane [35] at 60 °C in CH_3CN overnight gave **32**, **33**, and **34** in 87%, 40%, and 94% yield, respectively. The TBDMS-groups of **32**–**34** were removed by treatment with TBAF in THF for 2 h at room temperature to produce N4-carboranylalkyl-5-methyl-2′-deoxycytidine analogs **35**, **36**, **37** in 86%, 95%, and 97% yield, respectively. Compounds **32**–**37** were purified by silica gel chromatography.

2.2. Biological studies

PTAs of **1**, **2**, **3**, **4**, **9**, **16**–**22**, **28**–**30** and **35**–**37** were carried out using [γ-^{32}P]ATP as the phosphate donor and recombinant hTK1 as described previously [29,31]. 5′-Monophosphorylated products of the test compounds were detected by β-radiography of polyethylenimine (PEI)-cellulose chromatograms that were developed from small quantities of assay mixtures (Fig. 2 and S2/

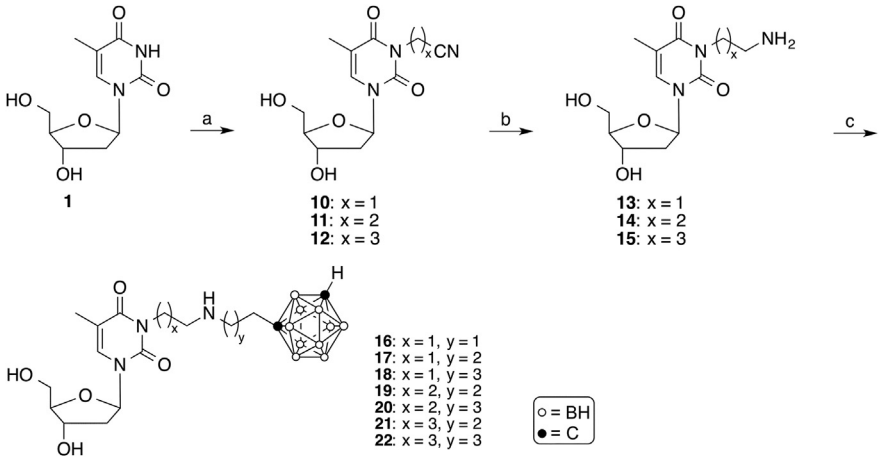

Scheme 2. Synthesis of compounds **16**–**22**. Reagents and conditions: (a) Iodoacetonitrile, 3-bromopropionitrile, or 4-bromobutanenitrile, K_2CO_3, DMF/acetone (1/1, v/v), 8 h, 60 °C; (b) KBH_4, Raney nickel, EtOH, rt; (c) 1-(2-iodoethyl)-*closo*-1,7-carborane [35], 1-(3-iodopropyl)-*closo*-1,7-carborane [35], or 1-(4-iodobutyl)-*closo*-1,7-carborane [35], NaH, DMF, 2 h, 90 °C.

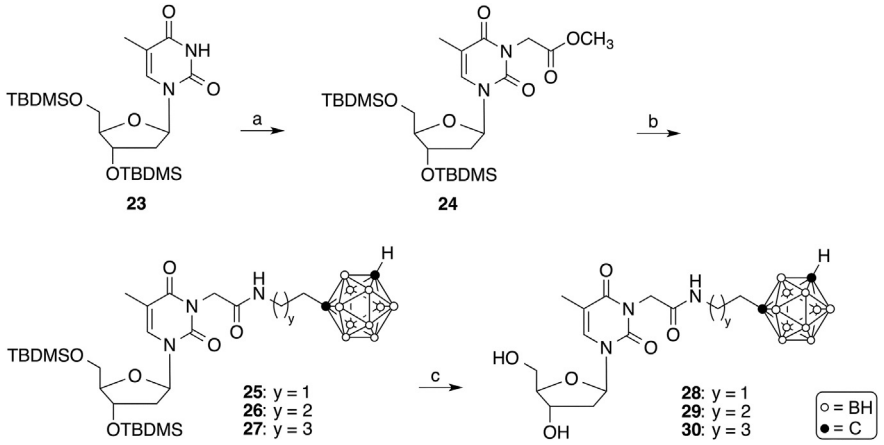

Scheme 3. Synthesis of compounds **28**–**30**. Reagents and conditions: (a) Methyl bromoacetate, acetone, NaH, 2 h, rt; (b) 1-(2-aminoethyl)-*closo*-1,7-carborane [35], 1-(3-aminopropyl)-*closo*-1,7-carborane [35], or 1-(4-aminobutyl)-*closo*-1,7-carborane [35], 1,2,4-triazole, DBU, 72 h, 80 °C; (c) TBAF, THF, rt, 2 h.

Supplementary Materials [SM]). The phosphorylation rates of the all test compounds are expressed relative to that of **1**, the natural substrate of TK1 (Table 1, Fig. 2). We have used such relative phosphorylation rates (rPRs) previously to establish preliminary SARs for larger 3CTA libraries [29,31]. Relative PRs do not reflect 100% accurately the enzyme kinetic properties of test compounds and they provide, if at all, little information about their enzyme inhibitory capacities [29,31]. Both properties are important to judge the potential of carboranyl pyrimidine nucleoside analogs as boron delivery agents for BNCT. Therefore, compounds **2**, **3**, **4**, and **21** and **22**, which were both stable and had high rPRs, were further evaluated in detailed enzyme kinetic- and inhibitory studies to obtain K_m, k_{cat}, rk_{cat}/K_m (k_{cat}/K_m relative to that of **1**) and IC_{50} of inhibition values (Table 1) [29].

The obtained rPRs for **3** and **4** were about twice as high as that of **2** (78.7 and 79.4% vs. 40.0%) and were in accordance with

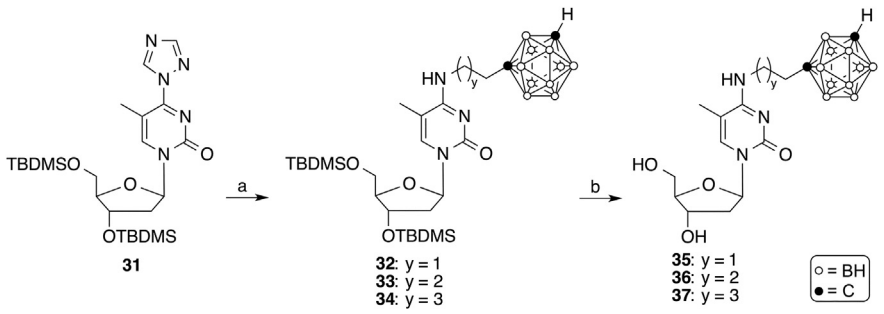

Scheme 4. Synthesis of compounds **35**–**37**. Reagents and conditions: (a) 1-(2-Aminoethyl)-*closo*-1,7-carborane [35], 1-(3-aminopropyl)-*closo*-1,7-carborane [35], or 1-(4-aminobutyl)-*closo*-1,7-carborane [35], CH_3CN, overnight, 60 °C; (b) TBAF, THF, rt, 2 h.

previously reported rPRs for both compounds [31]. Compounds **16**–**18**, with $-(CH_2)_2-NH-(CH_2)_{2,3,4}-$ spacer had rPRs ranging form 24.5–44.4%. These compounds proved to be unstable during storage in aqueous solutions even at −20 °C within 5–7 days. Among the compounds that were found to be stable during storage, compounds **21** and **22**, having $-(CH_2)_4-NH-(CH_2)_3-$ and $-(CH_2)_4-NH-(CH_2)_4-$ spacer, respectively, between carborane and scaffold of **1**, had rPRs comparable to that of **2** (45% and 38% vs. 40%), whereas the rPRs of compounds **19**, **20** and **28**–**30** were markedly lower (Table 1). A preliminary PTA for compound **9** resulted in a rPR of ~30% (SM, S.2). Interestingly, N4-carboranylalkyl-5-methyl-2′-deoxycytidine analogs **35**–**37** were not substrates of TK1 (data not shown). Overall, there was no clear SAR pattern among compounds **9**, **16**–**22** and **28**–**30**. If at all, the amido-substituted **28**–**30** had slightly lower rPRs than the amino-substituted **9** and **16**–**22**.

Using rPRs and stability as selection criteria, in-depth enzyme kinetic studies were carried out for compounds **1**, **2**, **3**, **4**, **21** and **22** using methods previously described by us (Table 1) [29]. The rk_{cat}/K_m values of **3** and **4** were 2.7–3.7 times higher than that of **2** (15.7% and 21.6% vs. 5.8%) whereas those of **21** (2.0%) and **22** (3.7%) were markedly lower. Furthermore, competitive inhibition studies were carried for **3**, **4**, **21** and **22** to determine IC_{50} values for their ability to compete for phosphorylation with **1** at the substrate-binding site of TK1 (Table 1) [29]. The obtained values were compared with those of **1** and **2**. The IC_{50} values for **21** and **22** (>250 μM) indicated that these compounds did not effectively compete with **1**. In contrast, the IC_{50} values of **3** and **4** were 2.7–4.2 times lower than that of **2** (13.5 μM and 8.9 μM vs. 37.5 μM).

Table 1
rPR, rK_{cat}/K_M, and IC_{50} values of **1**–**4**, **16**–**22**, and **28**–**30**.

Compd	rPR[a] (%)	K_m (μM)	k_{cat} (s^{-1})	rk_{cat}/K_m (%)	IC_{50} (μM)
1	100	2.4 ± 0.7	8.6	100	2.0 ± 0.3
2	40.0 ± 11.2	24.3 ± 2.1	5.1	5.8	37.5 ± 6.3
3	78.7 ± 3.4	7.5 ± 3.2	5.9	21.6	13.5 ± 2.1
4	79.4 ± 7.8	10.7 ± 1.2	6.1	15.7	8.9 ± 2.2
16	35.2 ± 5.3	nd	nd	nd	nd
17	24.5 ± 7.8	nd	nd	nd	nd
18	44.4 ± 8.7	nd	nd	nd	nd
19	18.8 ± 4.8	nd	nd	nd	nd
20	19.5 ± 5.3	nd	nd	nd	nd
21	45.2 ± 3.8	80.1 ± 37.6	5.9	2.0	>250
22	38.0 ± 6.5	39.8 ± 10.4	5.4	3.7	>250
28	19.2 ± 4.5	nd	nd	nd	nd
29	14.5 ± 4.8	nd	nd	nd	nd
30	12.3 ± 8.7	nd	nd	nd	nd

[a] rPr: phosphorylation rate relative to that of dThd. SDs are based on at least three measurements. nd: not determined. The following compound concentrations were used: rPR values: 100 μM nucleoside analog and 100 μM ATP; K_m *and* k_{cat} values: 1.95–500 μM nucleoside analog and 100 μM ATP; IC_{50} values: 0.5 μM dThd, 5 mM ATP, and 0–250 μM nucleoside analog.

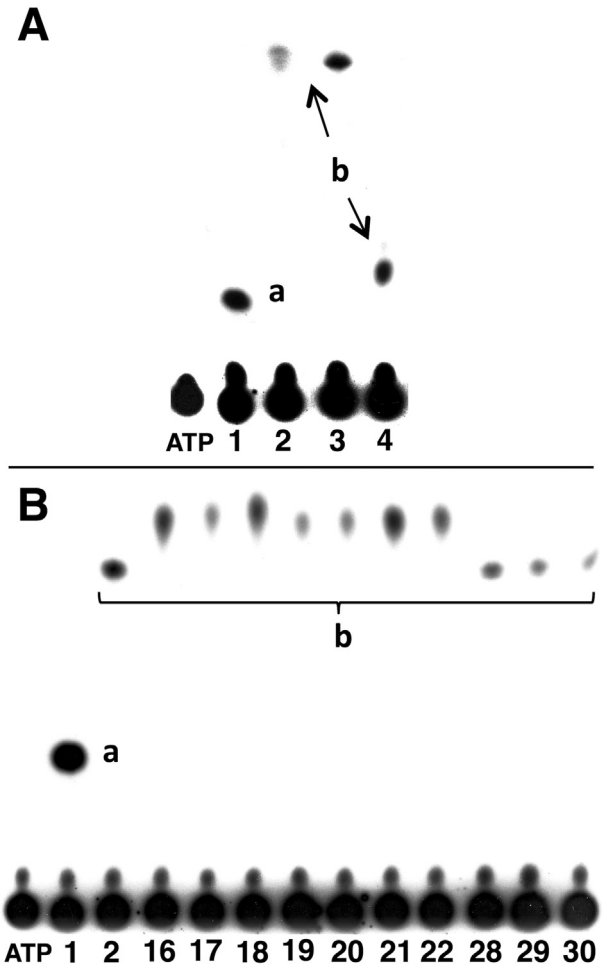

Fig. 2. A: β-Autoradiogram of a TLC analysis of the products from phosphate transfer assays using TK1 and [γ-^{32}P]ATP (phosphate donor) as well as **1**, **2**, **3**, and **4** as substrates. **B**: β-Autoradiogram of a TLC analysis of the products from phosphate transfer assays using TK1 and [γ-^{32}P]ATP (phosphate donor) as well as **1**, **2**, **16**–**22**, and **28**–**30** as substrates. a: Monophosphate of **1**; b; compound monophosphate.

Although **3** and **4** appeared to be equally effective as substrates and inhibitors of TK1, only **3** was initially selected for further *in vitro* and *in vivo* studies because **4** presumably is a mixture of two stable zwitterionic atropoisomers [11,31], as is evident from, e.g., the split signal for the H1'-proton in the ^{1}H NMR at 6.31 ppm and 6.39 ppm (SM, S3.3.1). In addition, it is conceivable that the charged character of these structures in this mixture impedes passive diffusion through cell membranes. Compound **3** was evaluated in qualitative *in vitro* and *in vivo* metabolomic HRMS studies using RG2 glioma cells and intracerebral RG2 tumors, respectively (Table 2). In addition, biodistribution studies were carried out in rats bearing intracerebral RG2 gliomas (Table 3). In both types of studies, **2** was used as a reference compound. The intracerebral RG2 glioma model was chosen for these studies because 3CTAs were initially designed and developed for BNCT of brain tumors *via* intracerebral (i.c.) injection [21]. The TK1 protein expression in RG2 cells appeared to be slightly higher than in TK(+) L929 cells, as determined by Western Blot analysis (Fig. 3). Both TK1(+) and TK1(−) L929 cells have been used previously by our group to analyze the intracellular formation of metabolites of **2** by radiodetection techniques [12].

In general, non-phosphorylated **2** and **3** could be detected both *in vitro* and *in vivo* samples by HRMS metabolomic analysis in both positive and negative ion mode (Table 2). In contrast, the corresponding monophosphates, **2-MP** and **3-MP**, were only measurable in negative ion mode. Di- and triphosphates of **2** and **3** could not be detected in either ion mode. The deviation of 12.5 ppm between calculated and found mass for **3-MP** *in vitro* is somewhat too high for accurate mass HRMS standards. However, the shape of the entire isotope pattern observed in this case is indicative for a **3-MP** metabolite (SM, S1.9.).

For a biodistribution study, **2** and **3** were administered intracerebrally (i.c.) by means of ALZET® pumps over a period of 24 h in rats bearing intracerebral RG2 gliomas, as described previously by us [21,22]. Rats were euthanized immediately thereafter and tumors, normal brain tissue, and blood were taken for boron determination by inductively coupled plasma-optical emission spectroscopy (ICP-OES). The results of this biodistribution study are summarized in Table 3. The boron concentration in brain tumors

Table 2
Accurate mass HRMS analysis of **2** and **3** and their monophosphate metabolites in RG2 cells and intracranial RG2 gliomas.[a]

Comp	Mode[b]	*In vitro*/*in vivo*	Molecular formula	Found[c] (*m*/*z*)	Calculated[d] (*m*/*z*)	Deviation (ppm)
2	Positive	*In vitro*	$C_{20}H_{40}N_2O_7B_{10} + H^+$	529.3941	529.3917	4.5
2	Negative	*In vitro*	$C_{20}H_{40}N_2O_7B_{10} - H^+$	527.3776	527.3760	3.0
2	Negative	*In vivo*	$C_{20}H_{40}N_2O_7B_{10} - H^+$	527.3782	527.3760	4.2
2-MP[e]	Negative	*In vitro*	$C_{20}H_{39}N_2O_{10}B_{10}P + K^+$	645.3022	645.2983	6.0
2-MP	Negative	*In vivo*	$C_{20}H_{39}N_2O_{10}B_{10}P + K^+$	645.2966	645.2983	2.6
3	Positive	*In vitro*	$C_{14}H_{29}N_3O_5B_{10} + H^+$	428.3195	428.3189	1.4
3	Negative	*In vitro*	$C_{14}H_{29}N_3O_5B_{10} + HCOO^-$	472.3078	472.3087	1.9
3	Negative	*In vivo*	$C_{14}H_{29}N_3O_5B_{10} + HCOO^-$	472.3108	472.3087	4.4
3-MP	Negative	*In vitro*	$C_{14}H_{28}N_3O_8B_{10}P + K^+$	544.2322	544.2254	12.5
3-MP	Negative	*In vivo*	$C_{14}H_{28}N_3O_8B_{10}P + K^+$	544.2249	544.2254	0.9

[a] See Supplementary materials for detailed measured and calculated isotope patterns.
[b] Negative and positive ion modes.
[c] Values corresponding to the most intense peak of the theoretical isotopic pattern.
[d] Most intense peak of the theoretical isotopic pattern. Calculated with Isotope Pattern Calculatorv 4.0 (http://yanjunhua.tripod.com/pattern1.htm).
[e] Monophosphate.

Table 3
Biodistribution of **2** and **3** in rats bearing intracerebral RG2 gliomas.[a]

Compd	Boron concentrations (μg/g)				Ratios	
	Tumor	R. brain	L. brain	Blood	T/B	T/Bl
2	8.8 ± 2.9	2.1 ± 0.9	1.3 ± 0.5	1.0 ± 0.4	4.3	9.3
3	32.5 ± 17.9	6.6 ± 8.4	1.5 ± 1.1	0.5 ± 0.03	4.9	62.5

[a] RG2 gliomas (10^5 cells/10 μL) were implanted stereotactically into the right caudate nucleus of syngeneic Fischer rats. Biodistribution studies were initiated 14 days subsequent to implantation. Quantities of **2** and **3** equivalent to 100 μg of boron, solubilized in 200 μL 35% aqueous DMSO, were administered i.c. in a volume of 200 μL by means of ALZET pumps (model#2001D) over 24 h at a flow rate of 8.33 μL/h. Rats were euthanized immediately thereafter, and their tumors, brains and blood were taken for boron determinations by ICP-OES. SDs are based on 4 animals per group.

exposed to **3** (32.5 μg boron (B)/g tumor) was about 4 times higher than that for **2** (8.9 μg B/g tumor). This difference reflects approximately the differences of TK1 substrate and inhibitor capacities between both compounds suggesting that intracellular entrapment of a monophosphate form of **3** is a factor contributing to its increased uptake in the tumor. Boron concentrations in the right and left cerebral hemispheres following administration of **3** were higher than those for **2** (6.6/1.5 μg B/g brain vs. 1.5/1.3 μg B/g brain). However, boron concentrations for both **2** and **3** in surrounding normal brain were significantly lower than in the TK1(+) proliferating tumor cells, as can be expected for non-dividing cells without

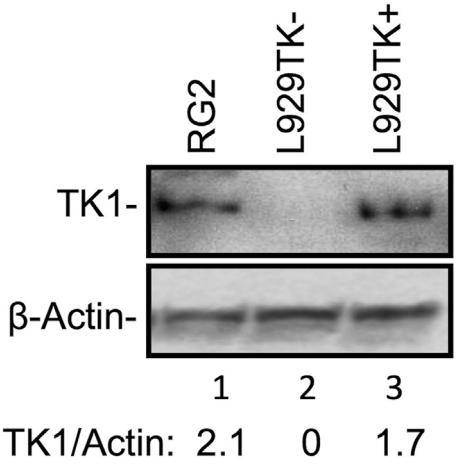

Fig. 3. Western blot analysis of the TK1 expression in RG2, TK1 (+) L929, and TK1 (−) L929 cells.

significant TK1 activity. The boron concentration in the blood was lower than in the tumor and in normal brain (0.5 μg B/g blood vs. 1.0 μg B/g blood), resulting in tumor/blood ratio of 62.5 for **3** compared to 9.3 for **2.** The slight differences in uptake between the normal brain of the right and left cerebral hemispheres is explained by the mode of delivery; that is, direct administration to the same site that the tumor cells had been stereotactically implanted, i.e., the right caudate nucleus (see Section 4.2.4. for details). The fact that the boron concentrations were low or non-detectable in the left, non-tumor bearing cerebral hemisphere and the blood, indicated that there was little intracerebral transfer of the test agents to the blood or *via* the corpus collosum from the right to the left cerebral hemisphere.

3. Discussion

Design strategies applied in recent years by our group to improve the capacity of 3CTAs to bind to TK1 focused on the introduction of hydrogen bond donor/acceptors in a spacer element between the carborane cluster and the 3-position of the scaffold of **1** to re-establish hydrogen bonds between substrate and enzyme [11,29,30]. None of these previously evaluated 2nd generation 3CTAs was markedly superior to **2** as a TK1 substrate and inhibitor. Some of the introduced functional groups improved aqueous solubility and/or impeded compound stability [29]. In addition, despite significant differences in structures and also physicochemical properties, no clear-cut TK1 substrate SAR emerged for these 3CTAs [11]. Similar results were obtained for compounds **9**, **16**–**22**, and **28**–**30**, having amino- and amido groups in the linker between carborane and **1**. Moving the carboranylalkylamino-substituent from the 3- to the 4-position of the pyrimidine nucleoside scaffold, as in compounds **35**–**37**, abolished TK1 substrate characteristics. Lesnikowski et al. recently reported similar observations for a series of triazolo- and ether modified carboranyl pyrimidine nucleoside analogs [13].

A detailed analysis of their kinase interacting properties showed that both **3** and **4** were ~3–4 times better substrates and inhibitors of TK1 than **2**. This is the first SAR study clearly identifying 2nd generation 3CTAs with markedly improved activity compared with 1st generation **2**. Biodistribution studies with rats bearing intracerebral RG2 glioma, resulting in a tumor to blood ratio of ~62 for **3** compared to ~9 for **2**, seemed to reflect this superiority.

Metabolomic HRMS studies showed that **2** and **3** were monophosphorylated to **2-MP** and **3-MP**, respectively, in TK1(+) RG2 cells, both *in vitro* and *in vivo*. In addition, non-phosphorylated **2** and **3** were detected in both types of biological samples, whereas the di- and triphosphates of both 3CTAs were not found. These

results confirm the recently reported analysis of the intracellular formation of metabolites of **2** in TK1(+)- and TK1(−) L929 cells by radiodetection techniques [12], which showed production of tritiated **2-MP** in TK1(+) L929 cells but not in their TK1(−) L929 counterparts. Di- and triphosphorylation did not seem to occur in the TK1(+) L929 cells but a significant quantities of tritiated **2** was found in both cells variants. Therefore, it is conceivable that mechanisms other than phosphorylation contribute to the tumor-selective accumulation of 3CTAs, such as **2** and **3**.

The most important consequence of the results presented here is that they challenge the current hypothesis for the design of 3CTAs. It seems that depending on an appropriate spacer length between carborane cage and nucleoside scaffold in 3CTAs, the cluster is actually located within the substrate-binding pocket. Furthermore, a single amino substituent at the cluster appeared to interact with amino acid residues within the substrate-binding site leading to markedly enhanced TK1 binding affinity and, thus, improved substrate characteristics and more effective competition with **1**. This indicates that the use of the carborane scaffold as a 3D-platform for the introduction of additional/different substituents can lead to 3rd generation 3CTAs with further enhanced TK1 substrate/inhibitor capacities.

Another potential application of 3CTAs in cancer therapy could be that of TK1 inhibitors used in combination with DNA damaging γ-radiation or chemotherapeutics. Recent studies have demonstrated that DNA damage results in increased TK1 expression especially in *p53*-deficient HCT-116 cancer cells [40]. TK1 expression proved to be nonessential for the growth of *p53*-deficient HCT-116 cells, but was important in providing sufficient triphosphate pools of **1** for DNA repair triggered by the genotoxic insult of these cells. Consequently, TK1 repression, for example *via* siRNA-mediated silencing, in *p53*-deficient HCT-116 cells caused an increase in cell death following DNA damage [40–42]. The apparent importance of TK1 for DNA repair, particularly in the context of *p53*-gene abnormalities, suggests the possible use of 3CTAs as inhibitors of TK1 in combination therapies, possibly even including BNCT, of cancer *via* systemic administration.

4. Experimental protocol

4.1. Chemistry

4.1.1. General conditions for chemical experiments

^{1}H and ^{13}C NMR spectra were obtained on a Bruker AVIII400HD NMR spectrometer or a Bruker DRX400 NMR spectrometer at The Ohio State University College of Pharmacy. Chemical shifts (δ) are reported in ppm from internal deuterated chloroform or deuterated methanol. Coupling constants are reported in Hz. ^{13}C NMR spectra are fully decoupled. Accurate- and high resolution mass spectra were obtained on a Waters Micromass LCT mass spectrometer or a Waters Micromass Q-TOF II mass spectrometer at The Ohio State University Campus Chemical Instrumentation Center, or a Waters Micromass Q-TOF micromass spectrometer at The Ohio State University College of Pharmacy. For all carborane-containing compounds, the found mass corresponding to the most intense peak of the theoretical isotopic pattern was reported. Measured patterns agreed with calculated patterns.

Silica gel 60 (0.063–0.200 mm), used for gravity column chromatography, and silica gel 60 (0.015–0.049 mm), used for flash column chromatograph, were purchased from Dynamic Adsorbents Inc. (Norcross, GA). Reagent-grade solvents were used for silica gel column chromatography. Precoated glass-backed TLC plates with silica gel 60 F254 (0.25-mm layer thickness) from Dynamic Adsorbents (Norcross, GA) were used for TLC. General compound visualization for TLC was achieved by UV light. Carborane-containing compounds were selectively visualized by spraying the plate with a 0.06% $PdCl_2$/1% HCl solution and heating at 120 °C, which caused the slow (15–45 s) formation of a gray spot due to the reduction of Pd^{2+} to Pd^{0}. Preparative HPLC purification was performed with a Gemini 5μ C18 column (21.20 mm × 250 mm, 5 μm particle size) supplied by Phenomenex Inc. CA, USA on a Hitachi HPLC system (L-2130) with a Windows based data acquisition and Hitachi Diode array detector (L-2455). Purification was accomplished using two different solvent systems: 1) 0.1% TFA in H_2O and 2) H_2O (0.1% TFA)/MeOH (0.1% TFA). The flow rate was 7 mL/min. Detailed gradient conditions for purification of specific compounds are provided in the following. Analytical HPLC was conducted using a Gemini 5μ C18 110A Column (250 mm × 4.6 mm) supplied by Phenomenex Inc. CA, USA using the Hitachi system used for preparative HPLC. Two different methods were used: 1) 0.1% TFA in H_2O, and 2) H_2O (0.1% TFA)/MeOH (0.1% TFA). The flow rate was 1 mL/min. For method 2 the following gradient was applied: 100 (H_2O): 0 (MeOH) to 0:100 over 20 min and from 0:100 to 100:0 over 10 min. HPLC-grade solvents were used for HPLC. All compounds used for biological studies had a purity >95% at 254 nm detection according to analytical HPLC (SM).

Anhydrous solvents were purchased directly either from Acros Organics (Morris Plains, NJ) or from Sigma Aldrich (Milwaukee, WI). THF was distilled from sodium and benzophenone indicator under argon. *closo*-1,7-Carborane was purchased from Katchem Ltd. (Prage, Czech Republic). Thymidine (**1**, Thd) was purchased from Chem-Impex International, Wood Dale, IL. Other chemicals used for synthesis were purchased from standard commercial vendors. 1-(2-Iodoethyl)-*closo*-1,7-carborane [35], 1-(3-iodopropyl)-*closo*-1,7-carborane [35], 1-(4-iodobutyl)-*closo*-1,7-carborane [35], 1-(2-aminoethyl)-*closo*-1,7-carborane [35], 1-(3-aminopropyl)-*closo*-1,7-carborane [35], and 1-(4-aminobutyl)-*closo*-1,7-carborane [35], as well as compounds **2** [32], **3** [31], **4** [31], **5** [34], **10** [29], **23** [37], and **31** [39] were synthesized according to previously described procedures. Spectroscopic data for compounds **2**–**5**, **10**, and **31** are provided in SM. Procedures for the syntheses of compounds **6** [43,44], **11** [45], **13** [46], **14** [47], and **15** [47] that are different from those described in this paper were reported previously. Unless specified otherwise, all reactions were carried out under argon atmosphere.

4.1.2. 3-Aminothymidine (**6**)

3′,5′-Diacetyl-3-nitrothymidine [34] (**5**) (2 g, 5.4 mmol) was dissolved in MeOH (130 mL) and added to the mixture of hydrazine hydrate (400 μL, 8.5 mmol) and 1 M KOH in 12 mL of MeOH and 25 mL H_2O. The reaction mixture was stirred at room temperature for 2 h. The solvent was removed under reduced pressure and the residue was purified by preparative HPLC (method 1). The solvent was evaporated under reduced pressure to afford a white amorphous solid. Retention time (analytical HPLC method 1): 28.9 min; yield: 400 mg, 28%. ^{1}H NMR (400 MHz, CD_3OD) δ 7.83 (q, J = 1.0 Hz 1H), 6.31 (t, J = 6.6 Hz, 1H), 4.57 (br.s, ~3H), 4.41 (dt, J = 3.5, 6.7 Hz, 1H), 3.93 (q, J = 3.5 Hz, 1H), 3.81 (dd, J = 3.2, 12.1 Hz, 1H), 3.74 (dd, J = 3.7 and 12.1 Hz, 1H), 2.17–2.40 (m, 2H), 1.95 (d, J = 1.2 Hz, 3H). ^{13}C NMR (100 MHz, CD_3OD) δ 161.92, 149.65, 134.19, 108.99, 87.96, 86.39, 71.02, 61.70, 40.44, 12.07. Accurate mass HRMS (ESI+): *m/z* calcd for $C_{10}H_{16}N_3O_5$ $(M + H)^+$ 258.1090, found 258.1099, 280.0905 $(M + Na)^+$, 296.0677 $(M + K)^+$.

4.1.3. 3-Amino-3′,5′-bis-O-(tert-butyldimethylsilyl)thymidine (**7**)

3-Aminothymidine (**6**) (500 mg, 2 mmol), *tert*-butyldimethylsilyl chloride (1.8 g, 11.5 mmol), and imidazole (0.75 g, 11.5 mmol) were dissolved in DMF (100 mL) and stirred overnight at room temperature. The solvent was evaporated under reduced pressure and the residue purified by silica gel column chromatography using a DCM/

MeOH solvent system. The product was obtained as a white amorphous solid at a solvent ratio of DCM/MeOH (24/1, v/v). R_f: 0.47 (DCM/MeOH, 24/1, v/v); yield; 0.8 g, 86%. ^{1}H NMR (400 MHz, $CDCl_3$) δ 7.42–7.46 (m, 1H), 6.32 (dd, J = 5.9, 7.5 Hz, 1H), 4.92 (br.s, ~1.5H), 4.37 (dt, J = 2.7, 5.7 Hz, 1H), 3.92 (q, J = 2.5 Hz, 1H), 3.85 (dd, J = 2.6, 11.4 Hz, 1H), 3.73 (dd, J = 2.6, 11.3 Hz, 1H), 2.27 (ddd, J = 2.8, 5.9, 13.1 Hz, 1H), 1.96–2.03 (m, 1H), 1.94 (s, 3H), 0.86 and 0.89 (two s, 18H), 0.045–0.079 (four s, 12H). ^{13}C NMR (100 MHz, $CDCl_3$) δ 160.55, 148.53, 132.30, 109.30, 88.07, 85.96, 72.22, 62.99, 41.74, 26.03, 25.84, 18.49, 18.10, 13.29, −4.53, −4.74, −5.28, −5.32. Accurate mass HRMS (ESI+): m/z calcd for $C_{22}H_{43}N_3NaO_5Si_2$ $(M + Na)^+$ 508.2639, found 508.2641.

4.1.4. 3′,5′-Bis-O-(tert-butyldimethylsilyl)-3-{[3-(closo-1,7-carboranyl)propyl]amino}thymidine (8)

A mixture of compound **7** (30 mg, 0.06 mmol), 1-(3-iodopropyl)-*closo*-1,7-carborane [35] (19 mg, 0.06 mmol), and NaH (3 mg, 0.12 mmol, 60% NaH in mineral oil) in DMF (2 mL) was stirred at 80 °C for 2 h. The solvent was evaporated and the residue was purified by silica gel column chromatography to give the product as a white amorphous solid. R_f: 0.72 (hexanes/EtOAc, 7/3, v/v); yield: 12.4 mg, 30%; ^{1}H NMR (400 MHz, $CDCl_3$) δ 7.47 (s, 1H), 6.32 (t, J = 7.2 Hz, 1H), 4.33–4.39 (m, 1H), 3.90–3.95 (m, 1H), 3.87 (dd, J = 2.3 and 11.5 Hz, 1H), 3.73 (dd, J = 2.1 and 11.5 Hz, 1H), 3.31–1.55 (br. m, 10H), 2.80–2.90 (m, 3H), 2.22–2.30 (m, 1H), 2.02–2.12 (m, 2H), 1.94–2.12 (m, 1H), 1.92 (s, 3H), 1.54–1.64 (m, 2H), 0.87 and 0.89 (two s, 18H), 0.05 and 0.08 (two s, 12H). ^{13}C NMR (100 MHz, $CDCl_3$) δ 162.1, 149.8, 133.33, 109.68, 88.1, 85.9, 75.9, 72.3, 63.1, 54.9, 49.3, 41.8, 34.4, 28.24, 26.1, 18.3, 13.4, −4.9. Accurate mass HRMS (ESI+): m/z calcd for $C_{27}H_{59}B_{10}N_3NaO_5Si_2$ $(M + Na)^+$ 692.4894, found 692.4912.

4.1.5. 3-{[3-(closo-1,7-Carboranyl)propyl]amino}thymidine (9)

A mixture of compound **8** (12 mg, 0.018 mmol) and TBAF (38 μL, 0.04 mmol, 1 M in THF) was stirred in THF (1 mL) for 2 h. The solvent was evaporated and the residue was purified by silica gel column chromatography to give the product as a white amorphous solid. R_f: 0.49 (DCM/MeOH, 9/1, v/v); yield: 5 mg, 63%. ^{1}H NMR (400 MHz, CD_3OD) δ 7.85 (s, 1H), 6.30 (t, J = 6.6 Hz, 1H), 4.34–4.43 (m, 1H), 3.89–3.95 (m, 1H), 3.80 (dd, J = 2.7 and 12.1 Hz, 1H), 3.73 (dd, J = 3.5 and 12.1 Hz, 2H), 3.49 (s, 1H), 2.83 (t, J = 6.9 Hz, 2H), 2.08–2.34 (m, 4H), 1.93 (s, 3H), 1.55–3.31 (br. m, 10H), 1.52–1.62 (m, 2H). ^{13}C NMR (100 MHz, CD_3OD) δ 164.0, 151.7, 136.0, 110.5, 88.9, 87.4, 77.7, 72.1, 62.7 56.87, 50.0, 41.4, 35.5, 29.1 13.1. Accurate mass HRMS (ESI+): m/z calcd for $C_{15}H_{31}B_{10}N_3NaO_5$ $(M + Na)^+$ 464.3165, found 464.3173.

4.1.6. General procedure for the synthesis of compounds 11 and 12

Thymidine (**1**) (5 g, 20.6 mmol) and potassium carbonate (8.5 g, 61.5 mmol) were dissolved in acetone/DMF (100 mL, 1/1, v/v) and cyanoalkyl halide (45 mmol) was added. The reaction mixture was stirred under reflux for 6 h, cooled to room temperature, added to H_2O (750 mL), and extracted with EtOAc (4 × 250 mL). The organic layer was separated, dried with anhydrous magnesium sulfate, evaporated under reduced pressure, and purified by silica gel column chromatography. The product was obtained as a white amorphous solid at a solvent ratio of DCM/MeOH (24/1, v/v).

4.1.6.1. 3-(2-Cyanoethyl)thymidine (11).

R_f: 0.70 (DCM/MeOH, 9/1, v/v), yield: 5.8 g, 97%. ^{1}H NMR (400 MHz, CD_3OD) δ 7.86 (s, 1H), 6.29 (t, J = 6.6 Hz, 1H), 4.36–4.44 (m, 1H), 4.21 (dt, J = 2.7 and 6.7 Hz, 2H), 3.88–3.96 (m, 1H), 3.80 (dd, J = 3.0 and 12.0 Hz, 1H), 3.73 (dd, J = 3.5 and 12.0 Hz, 1H), 2.82 (t, J = 6.7 Hz, 2H), 2.15–2.35 (m, 2H), 1.91 (s, 3H). ^{13}C NMR (100 MHz, CD_3OD) δ 165.09, 152.16, 137.02, 119.04, 110.80, 88.99, 87.31, 72.16, 62.86, 41.45, 37.93, 16.64, 13.32. Accurate mass HRMS (ESI+): m/z calcd for $C_{13}H_{17}N_3NaO_5$ $(M + Na)^+$ 318.1066, found 318.1033, 334.0800 $(M + K)^+$.

4.1.6.2. 3-(3-Cyanopropyl)thymidine (12).

R_f: 0.70 (DCM/MeOH, 9/1, v/v), yield: 5.0 g, 80%. ^{1}H NMR (400 MHz, CD_3OD) δ 7.85 (s, 1H), 6.29 (t, J = 6.6 Hz, 1H), 4.36–4.44 (m, 1H), 4.05 (t, J = 6.7 Hz, 2H), 3.91 (q, J = 3.3 Hz, 1H), 3.80 (dd, J = 3.1 and 12.0 Hz, 1H), 3.73 (dd, J = 3.6 and 12.0 Hz, 1H), 2.50 (t, J = 7.0 Hz, 2H), 2.16–2.34 (m, 2H), 1.92–2.02 (m, 2H), 1.91 (s, 3H). ^{13}C NMR (100 MHz, CD_3OD) δ 165.66, 152.57, 136.79, 121.02, 110.78, 88.98, 87.29, 72.13, 62.86, 41.49, 41.34, 24.98, 15.55, 13.41. Accurate mass HRMS (ESI+): m/z calcd for $C_{14}H_{19}N_3NaO_5$ $(M + Na)^+$ 332.1222, found 332.1195.

4.1.7. General procedure for the synthesis of compounds 13–15

Potassium borohydride (2 g, 36 mmol) and Raney nickel (~600 mg) were dissolved in anhydrous ethanol (50 mL) [36]. 3-Cyanoalkylthymidine (**10**–**12**) (3.6 mmol) was added to the reaction mixture, which was stirred for 2 h at room temperature. The solvent was evaporated under reduced pressure and the residue was purified by preparative HPLC using solvent system 2 with the following gradient: 100 (H_2O/TFA):0 (MeOH/TFA) for 15 min, 100:0 to 50:50 over 75 min, and from 50:0 to 100:0 over the following 10 min. The solvents were evaporated under reduced pressure to afford a white amorphous solid.

4.1.7.1. 3-(2-Aminoethyl)thymidine (13).

R_f: 0.10 (DCM/MeOH, 17/3, v/v), retention time (preparative HPLC): 33–42 min, yield: 0.68 g, 67%. ^{1}H NMR (400 MHz, CD_3OD) δ 7.86 (s, 1H), 6.28 (t, J = 6.6 Hz, 1H), 4.34–4.40 (m, 1H), 4.20 (t, J = 5.2 Hz, 2H), 3.86–3.92 (m, 1H), 3.77 (dd, J = 2.9 and 12.0 Hz, 1H), 3.70 (dd, J = 3.4 and 12.0 Hz, 1H), 3.18 (t, J = 5.2 Hz, 2H), 2.15–2.30 (m, 2H), 1.89 (s, 3H). ^{13}C NMR (100 MHz, CD_3OD) δ 165.76, 152.87, 136.88, 110.99, 88.85, 87.19, 72.10, 62.80, 41.07, 40.03, 39.73, 13.15. Accurate mass HRMS (ESI+): m/z calcd for $C_{12}H_{20}N_3O_5$ $(M + H)^+$ 286.1403, found 286.1388, 324.0936 $(M + K)^+$.

4.1.7.2. 3-(3-Aminopropyl)thymidine (14).

R_f: 0.10 (DCM/MeOH, 17/3, v/v), retention time (preparative HPLC): 30–48 min, yield: 0.83 g, 82%. ^{1}H NMR (400 MHz, CD_3OD) δ 7.89 (s, 1H), 6.31 (t, J = 6.6 Hz, 1H), 4.36–4.42 (m, 1H), 4.04 (t, J = 6.4 Hz, 2H), 3.86–3.94 (m, 1H), 3.80 (dd, J = 2.9 and 12.0 Hz, 1H), 3.73 (dd, J = 3.5 and 12.0 Hz, 1H), 2.95 (t, J = 7.0 Hz, 2H), 2.15–2.32 (m, 2H), 1.94–2.04 (m, 2H), 1.92 (s, 3H). ^{13}C NMR (100 MHz, CD_3OD) δ 165.80, 152.69, 136.99, 110.90, 89.09, 87.34, 72.28, 62.91, 41.39, 39.11, 38.43, 27.07, 13.31. Accurate mass HRMS (ESI+): m/z calcd for $C_{13}H_{22}N_3O_5$ $(M + H)^+$ 300.1559, found 300.1549, 322.1449 $(M + Na)^+$.

4.1.7.3. 3-(4-Aminobutyl)thymidine (15).

R_f: 0.10 (DCM/MeOH, 17/3, v/v), retention time (preparative HPLC): 38–60 min, yield: 0.80 g, 79%. ^{1}H NMR (400 MHz, CD_3OD: δ 7.84 (s, 1H), 6.29 (t, J = 6.6 Hz, 1H), 4.38–4.44 (m, 1H), 3.90–4.00 (m, 3H), 3.80 (dd, J = 3.0 and 12.0 Hz, 1H), 3.74 (dd, J = 3.7 and 12.0 Hz, 1H), 3.95 (t, J = 6.7 Hz, 2H), 2.16–2.34 (m, 2H), 1.89 (s, 3H), 1.58–1.72 (br s, 4H). ^{13}C NMR (100 MHz, CD_3OD) δ 165.65, 152.51, 136.77, 110.03, 88.95, 87.25, 72.30, 62.95, 41.76, 41.33, 40.82, 26.78, 26.81, 13.56. Accurate mass HRMS (ESI+): m/z calcd for $C_{14}H_{24}N_3O_5$ $(M + H)^+$ 314.1716, found 314.1698, 336.1479 $(M + Na)^+$.

4.1.8. General procedure for the synthesis of compounds 16–22

Compounds **13**–**15** (0.18 mmol), iodoalkyl-*closo*-1,7-carborane [35] (0.18 mmol), and NaH (13 mg, 0.54 mmol, 60% in mineral oil) were dissolved in anhydrous DMF (2 mL) and stirred for 2 h at 80 °C. Following the addition of 100 μL H_2O the reaction mixture was purified by preparative HPLC using solvent system 2 with the following gradient: 80 (H_2O/TFA):20 (MeOH/TFA) to 0:100 over

90 min and from 0:100 to 100:0 over next 10 min. The solvents were evaporated under reduced pressure to afford a white amorphous solid.

*4.1.8.1. 3-({2-[2-(closo-1,7-Carboranyl)ethyl]amino}ethyl)thymidine (**16**).* R_f: 0.71 (DCM/MeOH, 4/1, v/v), retention time (preparative HPLC): 45–48 min, yield: 3 mg, 4%. ^{1}H NMR (400 MHz, CD_3OD) δ 7.93 (s, 1H), 6.33 (t, J = 6.7 Hz, 1H), 4.38–4.44 (m, 1H), 4.20–4.26 (m, 2H), 3.92–3.96 (m, 1H), 3.81 (dd, J = 2.9 and 12.0 Hz, 1H), 3.74 (dd, J = 3.3 and 12.0 Hz, 1H), 3.60–3.70 (m 3H), 3.02–3.10 (m, 2H), 2.30–2.40 (m, 2H), 2.20–2.30 (m, 2H), 1.94 (s, 3H), 1.55–3.31 (br. m, 10H). Accurate mass HRMS (ESI+): *m/z* calcd for $C_{16}H_{33}B_{10}N_3O_5$ $(M + H)^+$ 456.3502, found 456.3539, 478.3349 $(M + Na)^+$.

*4.1.8.2. 3-({2-[3-(closo-1,7-Carboranyl)propyl]amino}ethyl)thymidine (**17**).* R_f: 0.71 (DCM/MeOH, 4/1, v/v), retention time (preparative HPLC): 44–50 min, yield: 6 mg, 7%. ^{1}H NMR (400 MHz, CD_3OD) δ 7.92 (s, 1H), 6.33 (t, J = 6.7 Hz, 1H), 4.38–4.45 (m, 1H), 4.25 (t, J = 5.3 Hz, 2H), 3.93 (q, J = 3.1 Hz, 1H), 3.81 (dd, J = 3.1 and 12.0 Hz, 1H), 3.74 (dd, J = 3.5 and 12.0 Hz, 1H), 3.56 (s, 1H), 3.03 (t, J = 8.0 Hz, 2H), 2.95 (t, J = 7.7 Hz, 2H), 2.20–2.30 (m, 2H), 2.07 (t, J = 7.4 Hz, 2H), 1.94 (s, 3H), 1.65–1.85 (m, 2H), 1.55–3.31 (br. m, 10H). ^{13}C NMR (100 MHz, CD_3OD) δ 165.78, 152.90, 137.13, 111.01, 89.12, 87.34, 76.34, 72.31, 62.90, 57.93, 57.25, 43.63, 41.39, 39.07, 34.63, 26.34, 13.22. Accurate mass HRMS (ESI+): *m/z* calcd for $C_{17}H_{36}B_{10}N_3O_5$ $(M + H)^+$ 470.3658, found 470.3694.

*4.1.8.3. 3-({2-[4-(closo-1,7-Carboranyl)butyl]amino}ethyl)thymidine (**18**).* R_f: 0.71 (DCM/MeOH, 4/1, v/v), retention time (preparative HPLC): 50–54 min, yield: 10 mg, 12%. ^{1}H NMR (400 MHz, CD_3OD) δ 7.92 (s, 1H), 6.33 (t, J = 6.7 Hz, 1H), 4.38–4.45 (m, 1H), 4.26 (t, J = 5.0 Hz, 2H), 3.90–3.96 (m, 1H), 3.81 (dd, J = 3.1 and 12.0 Hz, 1H), 3.74 (dd, J = 3.5 and 12.0 Hz, 1H), 3.52 (s, 1H), 3.31 (m, 2H), 3.00 (t, J = 7.6 Hz, 2H), 2.20–2.35 (m, 2H), 2.00–2.10 (m, 2H), 1.94 (s, 3H), 1.55–1.65 (m, 2H), 1.55–3.31 (br. m, 10H), 1.40–1.50 (m, 2H). ^{13}C NMR (100 MHz, CD_3OD) δ 165.70, 152.85, 137.05, 110.93, 89.06, 87.26, 72.24, 71.90, 62.82, 57.02, 47.88, 41.32, 38.99, 37.40, 28.06, 26.76, 13.14. Accurate mass HRMS (ESI+): *m/z* calcd for $C_{18}H_{38}B_{10}N_3O_5$ $(M + H)^+$ 484.3815, found 484.3834.

*4.1.8.4. 3-({3-[3-(closo-1,7-Carboranyl)propyl]amino}propyl)thymidine (**19**).* R_f: 0.66 (DCM/MeOH, 17/3, v/v), retention time (preparative HPLC): 62–64 min, yield: 22 mg, 26%. ^{1}H NMR (400 MHz, CD_3OD) δ 7.92 (s, 1H, H-6), 6.32 (t, J = 6.7 Hz, 1H), 4.38–4.45 (m, 1H), 4.04 (t, J = 6.4 Hz, 2H), 3.88–3.94 (m, 1H), 3.81 (dd, J = 3.0 and 12.0 Hz, 1H), 3.74 (dd, J = 3.5 and 12.0 Hz, 1H), 3.51 (s, 1H), 2.90–3.04 (m, 4H), 2.18–2.32 (m, 2H), 1.98–2.10 (m, 2H), 1.92 (s, 3H), 1.55–3.31 (br. m, 10H), 1.40–1.60 (m, 4H). ^{13}C NMR (100 MHz, CD_3OD) δ 165.86, 152.68, 137.06, 110.90, 89.11, 87.31, 77.41, 72.26, 62.87, 57.08, 46.53, 41.43, 39.13, 37.55, 28.21, 26.97, 25.92, 13.38. Accurate mass HRMS (ESI+): *m/z* calcd for $C_{18}H_{38}B_{10}N_3O_5$ $(M + H)^+$ 484.3815, found 484.3837.

*4.1.8.5. 3-({3-[4-(closo-1,7-Carboranyl)butyl]amino}propyl)thymidine (**20**).* R_f: 0.71 (DCM/MeOH, 17/3, v/v), retention time (preparative HPLC): 62–70 min, yield: 26 mg, 30%. ^{1}H NMR (400 MHz, CD_3OD) δ 7.91 (s, 1H), 6.31 (t, J = 6.6 Hz, 1H), 4.38–4.45 (m, 1H), 4.04 (t, J = 6.4 Hz, 2H), 3.89–3.95 (m, 1H), 3.80 (dd, J = 3.0 and 12.0 Hz, 1H), 3.74 (dd, J = 3.5 and 12.0 Hz, 1H), 3.50 (s, 1H), 2.93–3.03 (m, 4H), 2.14–2.30 (m, 2H), 1.95–2.05 (m, 4H), 1.92 (s, 3H), 1.55–3.31 (br. m, 10H), 1.40–1.65 (m, 4H). ^{13}C NMR (100 MHz, CD_3OD) δ 165.84, 152.70, 137.06, 110.92, 89.13, 87.35, 77.41, 72.25, 62.88, 58.50, 53.17, 48.53, 41.43, 39.13, 37.55, 28.19, 26.95, 25.91, 13.33. Accurate mass HRMS (ESI+): *m/z* calcd for $C_{19}H_{40}B_{10}N_3O_5$ $(M + H)^+$ 498.3971, found 498.4001.

*4.1.8.6. 3-({4-[3-(closo-1,7-Carboranyl)propyl]amino}butyl)thymidine (**21**).* R_f: 0.63 (DCM/MeOH, 17/3, v/v), retention time (preparative HPLC): 58–68 min, yield: 42 mg, 48%. ^{1}H NMR (400 MHz, CD_3OD) δ 7.86 (s, 1H), 6.30 (t, J = 6.6 Hz, 1H), 4.38–4.45 (m, 1H), 3.90–4.00 (m, 3H), 3.80 (dd, J = 3.0 and 12.0 Hz, 1H), 3.73 (dd, J = 3.6 and 12.0 Hz, 1H), 3.52 (s, 1H), 3.00–3.10 (m, 2H), 2.92 (t, J = 7.6 Hz, 2H), 2.14–2.30 (m, 2H), 2.09 (t, J = 8.6 Hz, 2H), 1.92 (s, 3H), 1.65–1.85 (m, 6H), 1.55–3.31 (br. m, 10H). ^{13}C NMR (100 MHz, CD_3OD) δ 165.34, 152.28, 136.55, 110.66, 88.85, 87.04, 76.28, 72.09, 62.72, 56.98, 47.83, 43.41, 41.19, 41.16, 34.43, 27.67, 25.56, 24.39, 13.16. Accurate mass HRMS (ESI+): *m/z* calcd for $C_{19}H_{40}B_{10}N_3O_5$ $(M + H)^+$ 498.3971, found 498.3962.

*4.1.8.7. 3-({4-[4-(closo-1,7-Carboranyl)butyl]amino}butyl)thymidine (**22**).* R_f: 0.63 (DCM/MeOH, 17/3, v/v), retention time (preparative HPLC): 64–69 min, yield: 32 mg, 35%. ^{1}H NMR (400 MHz, CD_3OD) δ 7.87 (s, 1H), 6.31 (t, J = 6.6 Hz, 1H), 4.38–4.45 (m, 1H), 3.90–4.00 (m, 3H), 3.80 (dd, J = 3.0 and 12.0 Hz, 1H), 3.73 (dd, J = 3.6 and 12.0 Hz, 1H), 3.50 (s, 1H), 3.03 (t, J = 6.6 Hz, 2H), 2.97 (t, J = 7.6 Hz, 2H), 2.14–2.30 (m, 2H), 2.03 (t, J = 8.4 Hz, 2H), 1.91 (s, 3H), 1.65–1.75 (m, 4H), 1.55–1.65 (m, 2H), 1.55–3.31 (br. m, 10H), 1.42–1.52 (m, 2H). ^{13}C NMR (100 MHz, CD_3OD) δ 165.44, 152.37, 136.65, 110.75, 88.95, 87.14, 72.19, 62.81, 56.96, 49.90, 48.47 and 48.40, 41.29, 37.42, 28.06, 26.79, 25.69, 24.52, 13.23. Accurate mass HRMS (ESI+): *m/z* calcd for $C_{20}H_{42}B_{10}N_3O_5$ $(M + H)^+$ 512.4128, found 512.4112.

*4.1.9. 3′,5′-Bis-O-(tert-butyldimethylsilyl)-3-(methoxycarbonylmethyl)thymidine (**24**)*

A mixture of compound **23**[38] (1 g, 2.12 mmol), methyl bromoacetate (0.36 mL, 4.2 mmol), and sodium hydride (0.16 g, 6.8 mmol, 60% in mineral oil) were stirred in anhydrous acetone (5 mL) for 2 h at room temperature. H_2O (100 μL) was added to the reaction mixture, the solvents evaporated under reduced pressure, and the residue purified by silica gel chromatography using hexanes/EtOAc (4/1, v/v) as solvent system to afford a white amorphous solid. R_f: 0.58 (hexanes/EtOAc, 4/1, v/v), yield: 0.8 g, 69%. ^{1}H NMR (400 MHz, $CDCl_3$) δ 7.53 (s, 1H), 6.36 (dd, J = 5.9 and 7.8 Hz, 1H), 4.71 (s, 2H), 4.38–4.45 (m, 1H), 3.92–3.97 (m, 1H), 3.88 (dd, J = 2.6 and 11.4 Hz, 1H), 3.77–3.80 (m, 1H), 3.76 (s, 3H), 2.27 (ddd, J = 2.6, 5.7 and 13.1 Hz, 1H), 1.98–2.06 (m, 1H), 1.95 (s, 3H), 0.89 and 0.94 (two s, 18H), 0.08 and 0.12 (two s, 12H). ^{13}C NMR (100 MHz, $CDCl_3$) δ 168.39, 162.91, 150.56, 134.03, 110.93, 87.85, 85.61, 72.24, 62.97, 52.41, 41.92, 41.46, 25.92, 25.70, 18.38, 17.96, 13.19, −4.78, −5.43. Accurate mass HRMS (ESI+): *m/z* calcd for $C_{25}H_{46}N_2NaO_7Si_2$ $(M + Na)^+$ 565.2741, found 565.2738.

*4.1.10. General procedure for the synthesis of compounds **25**–**27***

A mixture of compound **24** (50 mg, 0.1 mmol), aminoalkyl-*closo*-1,7-carborane [35] (0.1 mmol), 1,2,4-triazole (2 mg, 0.03 mmol) and 1,8-diazabicyclo[5.4.0]undec-7-ene (5.4 μL, 0.036 mmol) were heated without solvent for 3 days at 80 °C. The reaction mixture was purified by silica gel chromatography using DCM/MeOH (19/1, v/v) as the solvent system to afford the desired product as a white amorphous solid.

*4.1.10.1. 3′,5′-Bis-O-(tert-butyldimethylsilyl)-3-({2-[2-(closo-1,7-carboranyl)ethyl]amino}-2-oxoethyl)thymidine (**25**).* R_f: 0.62 (DCM/MeOH, 19/1, v/v), yield: 7.4 mg, 12%. ^{1}H NMR (400 MHz, $CDCl_3$) δ 7.53 (s, 1H), 6.34 (dd, J = 5.9 and 7.7 Hz, 1H), 5.90 (t, J = 5.6 Hz, 1H), 4.57 (s, 2H), 4.38–4.43 (m, 1H), 3.93–3.96 (m, 1H), 3.87 (dd, J = 2.5 and 11.4 Hz, 1H), 3.76 (dd, J = 2.2 and 11.4 Hz), 3.20–3.30 (m, 2H), 2.93 (s, 1H), 2.22 (ddd, J = 2.5, 5.7 and 13.2 Hz, 1H), 2.18 (t, J = 7.4 Hz, 2H), 1.96–2.05 (m, 1H), 1.95 (s, 3H), 1.55–3.31 (br. m, 10H), 0.94 and 0.91 (two s, 18H), 0.08 and 0.12 (two s, 12H). ^{13}C NMR (100 MHz,

$CDCl_3$) δ 166.94, 163.22, 150.65, 134.18, 109.92, 87.86, 85.66, 72.22, 72.58, 62.96, 55.11, 43.93, 41.47, 39.13, 35.64, 25.71, 25.91, 17.96, 18.39, 13.20, -5.42, -4.77. Accurate mass HRMS (ESI+): *m/z* calcd for $C_{28}H_{59}B_{10}N_3NaO_6Si_2$ $(M + Na)^+$ 720.4843, found 720.4894.

*4.1.10.2. 3′,5′-Bis-O-(tert-butyldimethylsilyl)-3-({2-[3-(closo-1,7-carboranyl)propyl]amino}-2-oxoethyl)thymidine (**26**).* R_f: 0.64 (DCM/MeOH, 19/1, v/v), yield: 13 mg, 20%. ^1H NMR (400 MHz, CD_3OD) δ 7.63 (s, 1H), 6.28 (dd, *J* = 6.3 and 7.5 Hz, 1H), 4.54 (s, 2H), 4.45–4.51 (m, 1H), 3.92–3.98 (m, 1H), 3.89 (dd, *J* = 3.2 and 11.4 Hz, 1H), 3.83 (dd, *J* = 3.1 and 11.4 Hz, 1H), 3.47 (s, 1H), 3.14 (t, *J* = 6.6 Hz, 2H), 2.26 (ddd, *J* = 2.8, 5.9 and 13.3 Hz, 1H), 2.14–2.22 (m, 1H), 2.02 (t, *J* = 8.8 Hz, 2H), 1.93 (s, 3H), 1.55–3.31 (br. m, 10H), 1.53–1.66 (m, 2H), 0.94 and 0.96 (two s, 18H), 0.13 and 0.15 (two s, 12H). ^{13}C NMR (100 MHz, CD_3OD) δ 169.91, 165.03, 152.22, 136.07, 110.72, 89.36, 87.26, 73.82, 64.26, 56.90, 44.37, 41.96, 39.68, 35.28, 31.11, 26.33, 26.53, 18.93, 19.36, 13.44, −4.49, −5.17. Accurate mass HRMS (ESI+): *m/z* calcd for $C_{29}H_{61}B_{10}N_3NaO_6Si_2$ $(M + Na)^+$ 734.5000; found 734.5054.

*4.1.10.3. 3′,5′-Bis-O-(tert-butyldimethylsilyl)-3-({2-[4-(closo-1,7-carboranyl)butyl]amino}-2-oxoethyl)thymidine (**27**).* R_f: 0.63 (DCM/MeOH, 19/1, v/v), yield: 32 mg, 48%. ^1H NMR (400 MHz, $CDCl_3$) δ 7.52 (s, 1H), 6.35 (dd, *J* = 5.9 and 7.7 Hz, 1H), 5.87 (t, *J* = 5.2 Hz, 1H), 4.57 (s, 2H), 4.34–4.42 (m, 1H), 3.92–3.96 (m, 1H), 3.87 (dd, *J* = 2.4 and 11.4 Hz, 1H), 3.76 (dd, *J* = 2.2 and 11.4 Hz, 1H), 3.22 (q, *J* = 6.4 Hz, 2H), 2.90 (s, 1H), 2.27 (ddd, *J* = 2.4, 5.7 and 13.0 Hz, 1H), 1.96–2.06 (m, 3H), 1.94 (s, 3H), 1.55–3.31 (br. m, 10H), 1.24–1.46 (m, 4H), 0.89 and 0.93 (two s, 18H), 0.07 and 0.12 (two s, 12H). ^{13}C NMR (100 MHz, $CDCl_3$) δ 166.83, 163.21, 150.68, 134.06, 109.89, 87.81, 85.61, 72.20, 62.94, 54.77, 43.93, 41.44, 39.10, 36.39, 29.03, 27.11, 25.69, 25.90, 17.95, 18.37, 13.20, −5.44, −4.79. Accurate mass HRMS (ESI+): *m/z* calcd for $C_{30}H_{63}B_{10}N_3NaO_6Si_2$ $(M + Na)^+$ 748.5156, found 748.5128.

*4.1.11. General procedure for the synthesis of compounds **28**–**30***

THF (1 mL) was added to compounds **25**–**27** (0.034 mmol) and TBAF (75 μL, 1 M solution in THF, 0.075 mmol). The reaction mixture was stirred at room temperature for 2 h, the solvents were evaporated under reduced pressure, and the residue was purified by silica gel chromatography using DCM/MeOH, 9/1, v/v as solvent system to produce a white amorphous solid.

*4.1.11.1. 3-({2-[2-(closo-1,7-Carboranyl)ethyl]amino}-2-oxoethyl) thymidine (**28**).* R_f: 0.51 (DCM/MeOH, 9/1, v/v), yield: 15 mg, 93%. ^1H NMR (400 MHz, CD_3OD) δ 7.91 (s, 1H), 6.28 (t, *J* = 6.6 Hz, 1H), 4.53 (s, 2H), 4.37–4.44 (m, 1H), 3.89–3.94 (m, 1H), 3.81 (dd, *J* = 2.9 and 12.0 Hz, 1H), 3.72 (dd, *J* = 3.6 and 12.0 Hz, 1H), 3.53 (s, 1H), 3.20 (t, *J* = 7.9 Hz, 2H), 2.21–2.32 (m, 2H), 2.18 (t, *J* = 7.9 Hz, 2H), 1.92 (s, 3H), 1.55–3.31 (br. m, 10H). ^{13}C NMR (100 MHz, CD_3OD) δ 169.90, 165.26, 152.38, 137.03, 110.69, 89.02, 87.38, 72.13, 62.83, 57.28, 44.37, 41.51, 40.24, 36.58, 13.26. Accurate mass HRMS (ESI+): *m/z* calcd for $C_{16}H_{31}B_{10}NaN_3O_6$ $(M + Na)^+$ 492.3114, found 492.3158.

*4.1.11.2. 3-({2-[3-(closo-1,7-Carboranyl)propyl]amino}-2-oxoethyl) thymidine (**29**).* R_f: 0.54 (DCM/MeOH, 9/1, v/v), yield: 14 mg, 83%. ^1H NMR (400 MHz, CD_3OD) δ 7.90 (s, 1H), 6.29 (t, *J* = 6.5 Hz, 1H), 4.54 (s, 2H), 4.37–4.46 (m, 1H), 3.88–3.96 (m, 1H), 3.82 (dd, *J* = 2.8 and 12.0 Hz, 1H), 3.74 (dd, *J* = 3.3 and 12.0 Hz, 1H), 3.49 (s, 1H), 3.13 (t, *J* = 6.3 Hz, 2H), 2.21–2.34 (m, 2H), 2.02 (t, *J* = 8.3 Hz, 2H), 1.93 (s, 3H), 1.53–1.66 (m, 2H), 1.55–3.31 (br. m, 10H). ^{13}C NMR (100 MHz, CD_3OD) δ 169.93, 165.16, 152.31, 136.88, 110.61, 89.91, 87.25, 72.03, 62.74, 56.95, 44.33, 41.44, 39.70, 35.29, 31.04, 13.21. Accurate mass HRMS (ESI+): *m/z* calcd for $C_{17}H_{33}B_{10}N_3NaO_6$ $(M + Na)^+$ 506.3270, found 506.3274.

*4.1.11.3. 3-({2-[4-(closo-1,7-Carboranyl)butyl]amino}-2-oxoethyl) thymidine (**30**).* R_f: 0.47 (DCM/MeOH, 9/1, v/v), yield: 12 mg, 71%. ^1H NMR (400 MHz, CD_3OD) δ 7.90 (s, 1H), 6.29 (t, *J* = 6.5 Hz, 1H), 4.54 (s, 2H), 4.32–4.44 (m, 1H), 3.86–3.95 (m, 1H), 3.81 (dd, *J* = 2.7 and 12.0 Hz, 1H), 3.73 (dd, *J* = 3.3 and 12.0 Hz, 1H), 3.47 (s, 1H), 3.10–3.21 (m, 2H), 2.18–2.33 (m, 2H), 1.95–2.05 (m, 2H), 1.92 (s, 3H), 1.55–3.31 (br. m, 10H), 1.35–1.49 (m, 4H). ^{13}C NMR (100 MHz, CD_3OD) δ 169.88, 165.26, 152.40, 136.94, 110.69, 89.00, 87.32, 78.04, 72.12, 62.83, 56.96, 44.37, 41.51, 39.99, 37.85, 30.09, 28.47, 13.30. Accurate mass HRMS (ESI+): *m/z* calcd for $C_{18}H_{35}B_{10}N_3NaO_6$ $(M + Na)^+$ 520.3427, found 520.3444, 1017.7020 $(2M + Na)^+$.

*4.1.12. General procedure for the synthesis of compound **32**–**35***

A mixture of compound **31** [39] (52 mg, 0.1 mmol) and amino-alkyl-*closo*-1,7-carborane [35] (0.3 mmol) in anhydrous CH_3CN (2 mL) was refluxed overnight. The solvent was evaporated and residue was purified by silica gel column chromatography DCM/acetone (9/1, v/v) as the solvent system to produce a white amorphous solid.

*4.1.12.1. 3′,5′-Bis-O-(tert-butyldimethylsilyl)-N4-[2-(closo-1,7-carboranyl)ethyl]-5-methyl-2′-deoxycytidine (**32**).* R_f: 0.52 (DCM/acetone, 9/1, v/v), yield: 53 mg, 87%. ^1H NMR (400 MHz, $CDCl_3$) δ 7.59 (s, 1H), 6.32 (t, *J* = 6.7 Hz, 1H), 5.48 (br s, 1H), 4.37–4.44 (m, 1H), 3.92–3.73 (m, 3H), 3.48–3.57 (m, 2H), 2.97 (s, 1H), 2.32–2.42 (m, 1H), 2.29 (t, *J* = 7.3, 2H), 1.95–2.04 (m, 1H), 1.93 (s, 3H), 1.55–3.31 (br. m, 10H), 0.92 and 0.89 (two s, 18H), 0.11, 0.10, 0.07 and 0.06 (four s, 12H). ^{13}C NMR (100 MHz, $CDCl_3$) δ 163.87, 157.52, 139.14, 103.98, 90.11, 89.35, 87.71, 87.52, 73.44, 64.34, 56.89, 36.78, 32.50, 27.50, 27.26, 19.96, 19.51, 14.96, 14.66, −3.31, −3.76, −3.8, −3.83. Accurate mass HRMS (ESI+): *m/z* calcd for $C_{26}H_{58}B_{10}N_3O_4Si_2$ $(M + H)^+$ 640.4969, found 640.5021.

*4.1.12.2. 3′,5′-Bis-O-(tert-butyldimethylsilyl)-N4-[3-(closo-1,7-carboranyl)propyl]-5-methyl-2′-deoxycytidine (**33**).* R_f: 0.5 (DCM/acetone, 9/1, v/v), yield: 20 mg, 40%. ^1H NMR (400 MHz, $CDCl_3$) δ 7.51 (s, 1H), 6.38 (t, *J* = 6.25 Hz, 1H), 4.85 (br s, 1H), 4.36 (m, 1H), 3.84–3.92 (m, 2H), 3.76 (m, 1H), 3.47 (m, 2H), 2.90 (s, 1H), 2.36 (m, 1H), 1.93–2.02 (m, 3H), 1.88 (s, 3H), 1.66–1.68 (m, 2H), 1.55–3.31 (br. m, 10H), 0.92 and 0.88 (two s, 18H), 0.10, 0.09, 0.06 and 0.05 (four s, 12H). ^{13}C NMR (100 MHz, $CDCl_3$) δ 163.08, 156.22, 137.51, 101.20, 87.61, 85.81, 75.70, 71.83, 62.85, 55.07, 42.17, 40.15, 34.21, 30.21, 25.92, 18.56, 18.17, 13.29, −4.42, −4.74, −5.21, −5.26. Accurate mass HRMS (ESI+): *m/z* calcd for $C_{27}H_{59}B_{10}N_3O_4Si_2Na$ $(M + Na)^+$ 676.4945, found 676.4980.

*4.1.12.3. 3′,5′-Bis-O-(tert-butyldimethylsilyl)-N4-[4-(closo-1,7-carboranyl)butyl]-5-methyl-2′-deoxycytidine (**34**).* R_f: 0.56 (DCM/acetone, 9/1, v/v), yield: 60 mg, 94%. ^1H NMR (400 MHz, $CDCl_3$) δ 7.49 (s, 1H), 6.37 (t, *J* = 6.51 Hz, 1H), 4.95 (s, 1H), 4.35 (m, 1H), 3.83–3.93 (m, 2H), 3.75 (m, 1H), 3.49 (m, 2H), 2.89 (s, 1H), 2.35 (m, 1H), 1.90–2.00 (m, 3H), 1.87 (s, 3H), 1.48–1.56 (m, 2H), 1.55–3.31 (br. m, 10H), 1.33–1.44 (m, 2H), 0.91 and 0.87 (two s, 18H), 0.10, 0.09, 0.05 and 0.04 (four s, 12H). ^{13}C NMR (100 MHz, $CDCl_3$) δ 163.02, 156.18, 137.30, 101.31, 87.59, 85.78, 76.20, 71.81, 62.84, 54.99, 42.15, 40.70, 36.57, 28.93, 27.37, 25.95, 18.54, 18.16, 13.31, −4.43, −4.75, −5.22, −5.28. Accurate mass HRMS (ESI+): *m/z* calcd for $C_{28}H_{61}B_{10}N_3O_4Si_2Na$ $(M + Na)^+$ 691.5065, found 691.5049.

*4.1.13. General procedure for the synthesis of compounds **35**–**37***

Compounds **32**–**34** (0.08 mmol) were dissolved in THF (1 mL) and TBAF (0.17 mmol, 1 M solution in THF). The reaction mixture was stirred at room temperature for 2 h, the solvent evaporated under reduced pressure, and the residue was purified by silica gel chromatography using DCM/MeOH (9/1, v/v) as solvent system to produce a white amorphous solid.

*4.1.13.1. N4-[2-(closo-1,7-Carboranyl)ethyl]-5-methyl-2′-deoxycytidine (**35**).* R_f: 0.45 (DCM/MeOH, 9/1, v/v), yield: 27.6 mg, 86%. ^{1}H NMR (400 MHz, CD_3OD) δ 8.19 (s, 1H), 6.23 (t, J = 6.3 Hz, 1H), 4.41 (dt, J = 3.8, 7.2 Hz, 1H), 3.91–4.04 (m, 1H), 3.84 (dd, J = 2.9 and 12.1, 1H), 3.75 (dd, J = 3.3 and 12.1, 1H), 3.49–3.64 (m, 3H), 2.32–2.50 (m, 2H), 2.24 (m, 2H), 2.02 (s, 3H), 1.50–3.31 (br. m, 10H). ^{13}C NMR (100 MHz, CD_3OD) δ 160.39, 160.00, 158.73, 149.08, 140.89, 103.14, 88.53, 86.81, 73.09, 70.76, 61.44, 56.42, 42.22, 40.94, 34.46, 12.08. Accurate mass HRMS (ESI+): *m/z* calcd for $C_{14}H_{30}B_{10}N_3O_4$ $(M + H)^+$ 412.3239, found 412.3212.

*4.1.13.2. N4-[3-(closo-1,7-Carboranyl)propyl]-5-methyl-2′-deoxycytidine (**36**).* R_f: 0.47 (DCM/MeOH, 9/1, v/v), yield: 11.1 mg, 95%. ^{1}H NMR (400 MHz, CD_3OD) δ 8.18 (s, 1H), 6.23 (t, J = 6.3 Hz, 1H), 4.41 (dt, J = 3.8, 6.2 Hz, 1H), 3.97 (m, 1H), 3.84 (dd, J = 2.9, 12.1 Hz, 1H), 3.75 (dd, J = 3.3, 12.1 Hz, 1H), 3.53 (s, 1H), 3.38 (t, J = 7.4 Hz, 2H), 2.37 (ddd, J = 4.1, 6.2, 13.6 Hz, 1H), 2.24 (m, 1H), 2.09 (m, 2H), 2.03 (s, 3H), 1.71–1.81 (m, 2H), 1.50–3.31 (br. m, 10H). ^{13}C NMR (100 MHz, CD_3OD) δ 159.37, 149.56, 141.82, 103.97, 89.56, 87.78, 71.79, 62.48, 57.17, 43.19, 41.93, 34.91, 29.96, 13.11. Accurate mass HRMS (ESI+): *m/z* calcd for $C_{15}H_{32}B_{10}N_3O_4$ $(M + H)^+$ 426.3396, found 426.3378.

*4.1.13.3. N4-[4-(closo-1,7-Carboranyl)butyl]-5-methyl-2′-deoxycytidine (**37**).* R_f: 0.49 (DCM/MeOH, 9/1, v/v), yield: 36.8 mg, 97%. ^{1}H NMR (400 MHz, CD_3OD) δ 8.19 (s, 1H), 6.22 (t, J = 6.3 Hz, 1H), 4.41 (m, 1H), 3.97 (m, 1H), 3.84 (dd, J = 2.9, 12.1 Hz, 1H), 3.75 (dd, J = 3.5, 12.3 Hz, 1H), 3.46 (m, 3H), 2.32–2.40 (m, 1H), 2.20–2.28 (m, 1H), 1.97–2.09 (m, 5H), 1.50–3.31 (br. m, 10H), 1.54–1.65 (m, 2H), 1.42–1.52 (m, 2H). ^{13}C NMR (100 MHz, CD_3OD) δ 157.93, 148.09, 140.74, 102.90, 88.55, 86.71, 84.55, 76.60, 70.77, 61.45, 56.03, 54.26, 42.61, 41.77, 40.89, 36.59, 27.80, 27.28, 12.09. Accurate mass HRMS (ESI+): *m/z* calcd for $C_{16}H_{34}B_{10}N_3O_4$ $(M + H)^+$ 440.3552, found 440.3516.

4.2. Biology

4.2.1. Phosphate transfer assays (PTAs)

Compound **1**, **2**, **3**, **4**, **9**, **16**–**22**, **28**–**30**, and **35**–**37** were dissolved in DMSO (100 mM concentration) and further diluted with H_2O to produce stock solutions of concentrations (0.4 mM). The PTAs were carried out according to a previously reported procedure with minor modifications [29,31]. The reaction mixtures contained 100 μM nucleoside and 100 μM ATP (with a small fraction of 0.13 μM [γ-^{32}P]ATP (10 μCi/μL), 25 mM Tris–HCl (pH 7.6), 5 mM $MgCl_2$, 125 mM KCl, 10 mM DTT, and 0.5 mg/mL BSA in a total volume of 20 μL. [γ-^{32}P]ATP (specific activity: 3000 Ci/mmol) was obtained from Perkin Elmer, Waltham, MA. In all reactions, the final concentration of DMSO was set to <1%. The reaction mixtures were incubated at 37 °C for 20 min in the presence of 0.75 ng of TK1 (Biaffin GmbH & Co. KG, Kassel, Germany [specific activity: 1.7 U/mg − 1 Unit is defined as 1 μmol phosphate transferred to 3′-azido-3′-deoxythymidine per min]). Vials were heated for 2 min at 99 °C to deactivate the enzyme. The reaction mixtures were centrifuged and 2 μL supernatants were spotted on PEI–cellulose TLC plates (EMD Chemicals Inc.). The TLC plates were developed in a solvent system containing isobutyric acid:NH_4OH:H_2O (66:1:33) over a period of 6 h. The radiolabeled spots were visualized by placing the TLC plates on a BioMax XAR film (Kodak) overnight and developing the films using an X-ray film developer (Tiba M6B, Series VI B Rapid processor; Commonwealth X-Ray Inc.). The spot intensities of the phosphorylated compounds were calculated with Adobe Photoshop (Adobe Systems Incorporated, USA).

4.2.2. Enzyme kinetic studies (K_m and k_{cat})

The enzyme kinetics studies were carried out using the protocol described above for PTAs with varying concentrations of **1**, **2**, **3**, **4**, **21**, or **22** [29]. The reaction mixtures contained 1.95–500 μM nucleoside and 100 μM ATP (with a small fraction of 0.325 μM [γ-^{32}P]ATP (Perkin Elmer)), 25 mM Tris–HCl (pH 7.6), 5 mM $MgCl_2$, 125 mM KCl, 10 mM DTT, and 0.5 mg/mL BSA. The kinetic parameters were calculated with the enzyme kinetic module of SigmaPlot 12 (Systat Software Inc, USA) using the Michaelis–Menten equation.

4.2.3. Competitive TK1 inhibition studies (IC_{50} values)

The IC_{50} values were determined using a recently published procedure [29]. Compound **1** (0.5 μM) with [methyl-^{3}H]dThd (75 nM, 1 μCi/μL) was reacted with 5 mM ATP in presence of 0.75 ng of TK1, 25 mM Tris–HCl (pH 7.6), 5 mM $MgCl_2$, 10 mM DTT, and 0.5 mg/mL BSA in a total volume of 20 μL. [methyl-^{3}H]dThd (specific activity: 20 Ci/mmol) was obtained from Perkin Elmer, Waltham, MA. The reaction mixtures were incubated at 37 °C for 20 min in the presence of 0–250 μM of either **1**, **2**, **3**, **4**, **21**, or **22**. The reaction vials were centrifuged and supernatants (10 μL) were spotted on DE81 diethylaminoethanol (DEAE) filter paper (Whatman, USA). Dried filter papers were washed three times with ammonium formate buffer (5 mM) for 5 min and placed in elution buffer (0.5 mL, 0.1 M HCl and 0.2 M KCl). Scintillation cocktail (10 mL) (Fischer Scientific, Columbus, OH) was added and radioactivity was determined by scintillation counting. The IC_{50} values were determined with SigmaPlot 12 (Systat Software Inc, USA) using the four parameter logistic curve equation [y = min + {max − min}/{1 + (x/EC50)^(−Hillslope)}].

4.2.4. In vivo biodistribution studies

All animal studies were carried out in accordance with the *Guide for the Care and Use of Laboratory Animals* (National Academy Press, Washington, D.C., 1996) and approved by the Institutional Animal Care and Use Committee (IACUC) of The Ohio State University. The RG2 rat glioma (CRL-2433, American Type Culture Collection (ATCC), Manassus, VA) has been described in detail elsewhere [48]. Cells were propagated *in vitro* in T-75 flasks (Corning #430641) in Complete Dulbecco's Modified Eagle's Medium (DMEM; Life Technology Gibco, Grand Island, NY), high glucose formulation plus 10% Fetal Bovine Serum (FBS; Gemini Bio-Products, West Sacremento, CA) plus 1% penicillin/streptomycin (Gibco) (100 Units/mL penicillin and 100 μg/mL streptomycin) plus 1% L-glutamine (Gibco). Cells were harvested when they had reached confluency and were disaggregated by treatment with 0.5% trypsin (Sigma Biosciences, St. Louis, MO) and then washed in PBS (pH 7.4). Either 10^5 or 10^4 RG2 cells in 10 μL of DMEM were implanted stereotactically into the right caudate nucleus of syngeneic Fischer rats (Charles River, Cambridge, MA). Biodistribution studies were initiated 14 d later for rats receiving 10^5 cells and 15 d later for rats receiving 10^4 cells. Quantities of **2** and **3** equivalent to 100 μg of boron, solubilized in 200 μL of 35% aqueous DMSO, were administered intracerebrally (i.c.) by means of ALZET® osmotic pumps (model #2001D, Durect Corporation, Cupertino, CA), which had been implanted subcutaneously (s.c.) into the interscapular dorsal region of Fischer rats. The test agents were administered over 24 h at a flow rate of 8.33 μL/h *via* a catheter connected to a 28 gauge needle that had been inserted into the entry port of a plastic screw, which had been inserted into a burr hole in the calvarium prior to stereotactic implantation of the tumor cells. The test agents, therefore, were administered to the very same site as the tumor implantation in all animals. At the end of the administration period the rats were euthanized by exposure to CO_2 and immediately thereafter their brains were removed and blood samples were taken. The tumors

were carefully dissected out from the tumor bearing right cerebral hemisphere and normal brain and each weighed separately. Boron determinations were carried out, as previously described [49], except that ICP-OES was performed using an Agilent/Varian spectrometer (Santa Clara, CA). For metabolomic studies, the samples were placed into pre-weighed microcentrifuge tubes, weighed again, snap-frozen in liquid nitrogen, and then stored at −20 °C until MS analysis was performed at a later date.

4.2.5. Cell lines for in vitro studies

The cell lines used were the RG2 rat glioma (ATCC #CRL-2433), the L929 TK1(+) wild type cell line (ATCC #CCL1, NCTC clone 929) and its L929 TK1(−) mutant counterpart (ATCC #CCL1.3 L-M [TK-]), which do not express TK1. The TK1(−) phenotype was maintained by continuous culture in complete DMEM in the presence of 10 μM of 5-bromo-2'-deoxyuridine (Sigma Aldrich, St. Louis, MO).

4.2.6. In vitro studies

For *in vitro* metabolomic studies (see below), RG2 cells were grown to 80–90% confluency in T-75 flasks to an initial density of ~2.5 × 10^6 cells in 10 mL of complete DMEM as described earlier under '*In vivo biodistribution studies*'. In order to propagate the cells in medium free of **1**, they were washed with PBS, then treated in 10% dialyzed FBS in order to remove **1** from the media. Complete DMEM was removed and the cells were exposed for 2 h to either **2** or **3** at concentrations of 17.5 μM in 10 mL of DMEM free of compound **1** containing 10% dialyzed FBS (Gemini Bio-Products, Baltimore, MD). This was done in order to remove **1** from the cell culture medium. At the end of this treatment, the cell monolayers were washed with 5 mL of PBS (pH 7.4). Cells were disaggregated using a mixture of 0.5% trypsin and 0.2% EDTA-4Na (10× trypsin, Sigma's Biosciences) and this was terminated by adding an equal volume of media containing 10% dialyzed FBS as described above. Cells then were sedimented and resuspended in PBS. A small sample was taken for counting, and then the cells were transferred to pre-weighed microcentrifuge tubes and repetitively sedimented to remove the supernatant. Pellets were weighed, snap-frozen in liquid nitrogen, and stored frozen until analyzed by MS for metabolites of **2** and **3**.

4.2.7. Western blot studies

Western blot analysis was carried out on RG2 rat glioma, L929 TK1(+), and L929 TK1(−) cells. Cells were propagated and disaggregated as described above using complete DMEM. Cell lysates were prepared using T-PER tissue protein extraction reagent (Thermo Fisher Scientific, Waltham, MA). Proteins (25 mg) were resolved by electrophoresis on SDS-polyacrylamide gel (4–20%) and transferred on to polyvinylidine difluoride membranes (Bio-Rad Laboratories, Hercules, CA). Western blotting was performed using TK1 primary antibodies (Novus Biologicals, Littleton, CO) and anti-rabbit immunoglobulin G (IgG) horseradish peroxidase (HRP)-linked secondary antibodies (CellSignaling Technology Inc., Danvers, MA). The proteins recognized by the antibodies were visualized with SuperSignal West Dura Chemiluminescent Substrate (Thermo Fisher Scientific). Subsequently, the membranes were incubated with anti-beta actin antibodies for protein loading. The signal intensity of TK1 relative to beta-actin for each cell sample was determined by ImageJ and EXCEL.

4.2.8. Metabolomic studies

Samples included three dissected RG2 gliomas, two from rats that had received **3** (111 mg & 112 mg tumor wet weight) and one of which from a rat that received **2** (170 mg) as well as four pellets of RG2 cells from *in vitro* studies, two of which were exposed to **3** (54 mg & 51 mg cell net weight) and two were exposed to **2** (44 mg & 48 mg). Samples were lysed and metabolic activity was quenched by adding 1.0 mL of chilled 1:1 MeOH:H_2O mixture, followed by repetitive pipetting. The cell suspensions were vortexed and sonicated 3 x 10 s/ea. Metabolites were separated from cellular debris by centrifugation at 13 K rpm for 5 min at 4 °C. The supernatants were collected, dried in a vacufuge (Eppendorf, Hamburg, Germany) and re-suspended in 100 μL of H_2O with 2% CH_3CN for LC-MS injection. LC-MS experiments were performed on a Bruker maXis 4G high resolution mass spectrometer (Bremen, Germany) equipped with an electrospray source operated in both positive and negative ion modes. Accurate mass HRMS measurements (with coupled with the LC) were carried out by recalibrating the spectra using well-defined background ions. For comparison, theoretical isotope patterns were calculated with Isotope Pattern Calculator v4.0 (http://yanjunhua.tripod.com/pattern1.htm). ESI was carried out at a capillary voltage 4500 V and a source temperature of 200 °C. The nitrogen drying was set to 8.0 L/min and the nebulizer to 1 bar. The scan range was 100–1100 m/z. The HPLC system was a Dionex Ultimate 3000 (Thermo Fisher Scientific, Waltham, MA). Mobile phase A was H_2O containing 0.1% formic acid and mobile phase B was CH_3CN with 0.1% formic acid. A 2.1 × 50 mm Accucore Polar Premium column (Thermo Fisher Scientific) with a particle size of 2.6 μ was used for chromatographic separations. The gradient used was 0–80% B over 15 min with a flow rate of 200 μL/min. The total runtime was 26 min.

Acknowledgments

The authors thank Jeremy Keirsey and Nanette M. Kleinholz for carrying out the metabolomic experiments and Dr. Arpad Somogyi for helping with the interpretation of the obtained mass spectra. The metabolomic studies were done at the Campus Chemical Instrument Center, Mass Spectrometry and Proteomics Facility, The Ohio State University, Columbus, OH. The present studies were supported by funds from The Ohio State University College of Pharmacy and NIH grant R01 CA127935. The content is solely the responsibility of the authors and does not necessarily represent the official views of the National Institutes of Health.

Appendix A. Supplementary data

Supplementary data related to this article can be found at http://dx.doi.org/10.1016/j.ejmech.2015.05.042.

References

[1] E.S. Arner, S. Eriksson, Mammalian deoxyribonuclease kinases, Pharmacol. Ther. 67 (1995) 155–186.
[2] T. Yusa, Y. Yamaguchi, H. Ohwada, Y. Hayashi, N. Kuroiwa, T. Morita, M. Asanagi, Y. Moriyama, S. Fujimura, Activity of the cytosolic isozyme of thymidine kinase in human primary lung tumors with reference to malignancy, Cancer Res. 48 (1988) 5001–5006.
[3] M.P.B. Sandrini, A.R. Clausen, S.L.W. On, F.M. Aarestrup, B. Munch-Petersen, J. Piskur, Nucleoside analogues are activated by bacterial deoxyribonucleoside kinases in a species-specific manner, J. Antimicrob. Chemother. 60 (2007) 510–520.
[4] H. Saito, H. Tomioka, Thymidine kinase of bacteria: activity of the enzyme in actinomycetes and related organisms, J. Gen. Microbiol. 130 (1984) 1863–1870.
[5] M.P.B. Sandrini, O. Shannon, A.R. Clausen, L. Bjorck, J. Piskur, Deoxyribonucleoside kinases activate nucleoside antibiotics in severely pathogenic bacteria, Antimicrob. Agents Chemother. 51 (2007) 2726–2732.
[6] M.P.B. Sandrini, A.R. Clausen, B. Munch-Petersen, J. Piskur, Thymidine kinase diversity in bacteria, Nucleosides Nucleotides Nucleic Acids 25 (2006) 1153–1158.
[7] M. Hengstschlaeger, M. Knoefler, E.W. Muellner, E. Ogris, E. Wintersberger, E. Wawra, Different regulation of thymidine kinase during the cell cycle of normal versus DNA tumor virus-transformed cells, J. Biol. Chem. 269 (1994) 13836–13842.
[8] M. Hengstschlaeger, E.W. Muellner, E. Wawra, Thymidine kinase is expressed

differently in transformed versus normal cells: a novel test for malignancy, Int. J. Oncol. 4 (1994) 207–210.
[9] J.L. Sherley, T.J. Kelly, Regulation of human thymidine kinase during the cell cycle, J. Biol. Chem. 263 (1988) 8350–8358.
[10] E. De Clercq, Antiviral drugs in current clinical use, J. Clin. Virol. 30 (2004) 115–133.
[11] A. Khalil, K. Ishita, T. Ali, W. Tjarks, N3-substituted thymidine bioconjugates for cancer therapy and imaging, Future Med. Chem. 5 (2013) 677–692.
[12] E. Sjuvarsson, V.L. Damaraju, D. Mowles, M.B. Sawyer, R. Tiwari, H.K. Agarwal, A. Khalil, S. Hasabelnaby, A. Goudah, R.J. Nakkula, R.F. Barth, C.E. Cass, S. Eriksson, W. Tjarks, Cellular influx, efflux, and anabolism of 3-carboranyl thymidine analogs: potential boron delivery agents for neutron capture therapy, J. Pharmacol. Exp. Ther. 347 (2013) 388–397.
[13] B.A. Wojtczak, A.B. Olejniczak, L. Wang, S. Eriksson, Z.J. Lesnikowski, Phosphorylation of nucleoside-metallacarborane and carborane conjugates by nucleoside kinases, Nucleosides Nucleotides Nucleic Acids 32 (2013) 571–588.
[14] A. Ilinova, A. Semioshkin, I. Lobanova, V.I. Bregadze, A.F. Mironov, E. Paradowska, M. Studzinska, A. Jablonska, M. Bialek-Pietras, Z.J. Lesnikowski, Synthesis, cytotoxicity and antiviral activity studies of the conjugates of cobalt bis(1,2-dicarbollide)(-1) with 5-ethynyl-2'-deoxyuridine and its cyclic derivatives, Tetrahedron 70 (2014) 5704–5710.
[15] R.N. Grimes, Carboranes, second ed., Elsevier, Amsterdam, 2011.
[16] V.I. Bregadze, I.B. Sivaev, Polyhedral boron compounds for BNCT, in: N.S. Hosmane (Ed.), Boron Science. New Technologies and Applications, CRC Press, Boca Raton, FL, 2012, pp. 181–207.
[17] N.S. Hosmane, J.A. Maguire, Y. Zhu, M. Takagaki, Boron and Gadolinium Neutron Capture Therapy for Cancer Treatment, World Scientific Publishing Company, Singapore, 2012.
[18] R.F. Barth, M.G.H. Vicente, O.K. Harling, W.S. Kiger 3rd, J.K. Kent, J.P. Binns, M.F. Wagner, M. Suzuki, T. Aihara, I. Kato, S. Kawabata, Current status of boron neutron capture therapy of high grade gliomas and recurrent head and neck cancer, Radiat. Oncol. 7 (2012) 146.
[19] A.H. Soloway, W. Tjarks, B.A. Barnum, F.-G. Rong, R.F. Barth, I.M. Codogni, J.G. Wilson, The chemistry of neutron capture therapy, Chem. Rev. 98 (1998) 1515–1562.
[20] Y. Endo, T. Iijima, K. Yaguchi, E. Kawachi, N. Inoue, H. Kagechika, A. Kubo, A. Itai, Structure-activity study of retinoid agonists bearing substituted dicarba-closo-dodecaborane. Relation between retinoidal activity and conformation of two aromatic nuclei, Bioorg. Med. Chem. Lett. 11 (2001) 1307–1311.
[21] R.F. Barth, W. Yang, G. Wu, M. Swindall, Y. Byun, S. Narayanasamy, W. Tjarks, K. Tordoff, M.L. Moeschberger, S. Eriksson, P.J. Binns, K.J. Riley, Thymidine kinase 1 as a molecular target for boron neutron capture therapy of brain tumors, Proc. Natl. Acad. Sci. U. S. A. 105 (2008) 17493–17497.
[22] R.F. Barth, W. Yang, A.S. Al-Madhoun, J. Johnsamuel, Y. Byun, S. Chandra, D.R. Smith, W. Tjarks, S. Eriksson, Boron-containing nucleosides as potential delivery agents for neutron capture therapy of brain tumors, Cancer Res. 64 (2004) 6287–6295.
[23] W. Tjarks, R. Tiwari, Y. Byun, S. Narayanasamy, R.F. Barth, Carboranyl thymidine analogues for neutron capture therapy, Chem. Commun. (2007) 4978–4991.
[24] M. Welin, U. Kosinska, N.E. Mikkelsen, C. Carnrot, C. Zhu, L. Wang, S. Eriksson, B. Munch-Petersen, H. Eklund, Structures of thymidine kinase 1 of human and mycoplasmic origin, Proc. Natl. Acad. Sci. U. S. A. 101 (2004) 17970–17975.
[25] D. Segura-Pena, J. Lichter, M. Trani, M. Konrad, A. Lavie, S. Lutz, Quaternary structure change as a mechanism for the regulation of thymidine kinase 1-like enzymes, Structure 15 (2007) 1555–1566.
[26] U. Kosinska, C. Carnrot, M.P. Sandrini, A.R. Clausen, L. Wang, J. Piskur, S. Eriksson, H. Eklund, Structural studies of thymidine kinases from *Bacillus anthracis* and *Bacillus cereus* provide insights into quaternary structure and conformational changes upon substrate binding, FEBS J. 274 (2007) 727–737.
[27] Y. Byun, B.T.S. Thirumamagal, W. Yang, S. Eriksson, R.F. Barth, W. Tjarks, Preparation and biological evaluation of ^{10}B-enriched 3-[5-{2-(2,3-dihydroxyprop-1-yl)-o-carboran-1-yl}pentan-1-yl]thymidine (N5-2OH), a new boron delivery agent for boron neutron capture therapy of brain tumors, J. Med. Chem. 49 (2006) 5513–5523.
[28] R. Tiwari, A. Toppino, H.K. Agarwal, T. Huo, Y. Byun, J. Gallucci, S. Hasabelnaby, A. Khalil, A. Goudah, R.A. Baiocchi, M.V. Darby, R.F. Barth, W. Tjarks, Synthesis, biological evaluation, and radioiodination of halogenated closo-carboranylthymidine analogues, Inorg. Chem. 51 (2012) 629–639.
[29] H.K. Agarwal, C.A. McElroy, E. Sjuvarsson, S. Eriksson, M.V. Darby, W. Tjarks, Synthesis of N3-substituted carboranyl thymidine bioconjugates and their evaluation as substrates of recombinant human thymidine kinase 1, Eur. J. Med. Chem. 60 (2013) 456–468.
[30] S. Narayanasamy, B.T.S. Thirumamagal, J. Johnsamuel, Y. Byun, A.S. Al-Madhoun, E. Usova, G.Y. Cosquer, J. Yan, A.K. Bandyopadhyaya, R. Tiwari, S. Eriksson, W. Tjarks, Hydrophilically enhanced 3-carboranyl thymidine analogues (3CTAs) for boron neutron capture therapy (BNCT) of cancer, Bioorg. Med. Chem. 14 (2006) 6886–6899.
[31] Y. Byun, J. Yan, A.S. Al-Madhoun, J. Johnsamuel, W. Yang, R.F. Barth, S. Eriksson, W. Tjarks, Synthesis and biological evaluation of neutral and zwitterionic 3-carboranyl thymidine analogues for boron neutron capture therapy, J. Med. Chem. 48 (2005) 1188–1198.
[32] S. Hasabelnaby, A. Goudah, H.K. Agarwal, M.S. Abdalla, W. Tjarks, Synthesis, chemical and enzymatic hydrolysis, and aqueous solubility of amino acid ester prodrugs of 3-carboranyl thymidine analogs for boron neutron capture therapy of brain tumors, Eur. J. Med. Chem. 55 (2012) 325–334.
[33] X. Ariza, V. Bou, J. Vilarrasa, A new route to ^{15}N-labeled, N-alkyl, and N-amino nucleosides via N-nitration of uridines and inosines, J. Am. Chem. Soc. 117 (1995) 3665–3673.
[34] O. Gorchs, M. Hernandez, L. Garriga, E. Pedroso, A. Grandas, J. Farras, A new method for the preparation of modified oligonucleotides, Org. Lett. 4 (2002) 1827–1830.
[35] H.K. Agarwal, B. Buszek, K.G. Ricks, W. Tjarks, Synthesis of closo-1,7-carboranyl alkyl amines, Tetrahedron Lett. 52 (2011) 5664–5667.
[36] B. Wu, J. Zhang, M. Yang, Y. Yue, L.-J. Ma, X.-Q. Yu, Raney Ni/KBH_4. An Efficient and Mild System for the Reduction of Nitriles to Amines, ARKIVOC, Gainesville, FL, U.S., 2008, pp. 95–102.
[37] K. Yamada, Y. Hattori, T. Inde, T. Kanamori, A. Ohkubo, K. Seio, M. Sekine, Remarkable stabilization of antiparallel DNA triplexes by strong stacking effects of consecutively modified nucleobases containing thiocarbonyl groups, Bioorg. Med. Chem. Lett. 23 (2013) 776–778.
[38] X. Yang, V.B. Birman, Acyl transfer catalysis with 1,2,4-triazole anion, Org. Lett. 11 (2009) 1499–1502.
[39] H.J. Jessen, W. Fendrich, C. Meier, Synthesis and properties of fluorescent cycloSal nucleotides m^5K and its 2′,3′-dideoxy analog dm^5K, Eur. J. Org. Chem. (2006) 924–931.
[40] Y.-L. Chen, S. Eriksson, Z.-F. Chang, Regulation and functional contribution of thymidine kinase 1 in repair of DNA damage, J. Biol. Chem. 285 (2010) 27327–27335.
[41] T. Radivoyevitch, Y. Sauntharajah, J. Pink, G. Ferris, I. Lent, M. Jackson, D. Junk, C.A. Kunos, dNTP supply gene expression patterns after p53 loss, Cancers 4 (2012) 1212–1224.
[42] C.-M. Hu, Z.-F. Chang, Synthetic lethality by lentiviral short hairpin RNA silencing of thymidylate kinase and doxorubicin in colon cancer cells regardless of the p53 status, Cancer Res. 68 (2008) 2831–2840.
[43] K. Kohda, I. Kobayashi, K. Itano, S. Asano, Y. Kawazoe, Syntheses and properties of N-aminopyrimidines, Tetrahedron 49 (1993) 3947–3958.
[44] N. Ashida, S. Asano, K. Kohda, 3-Aminothymidine inhibits growth of cultured human T-cell acute lymphoblastoid leukemia cells, Anticancer Res. 14 (1994) 2061–2062.
[45] T. Umemoto, T. Wada, Nitromethane as a scavenger of acrylonitrile in the deprotection of synthetic oligonucleotides, Tetrahedron Lett. 46 (2005) 4251–4253.
[46] M.D. Bartholoma, A.R. Vortherms, S. Hillier, B. Ploier, J. Joyal, J. Babich, R.P. Doyle, J. Zubieta, Synthesis, cytotoxicity, and insight into the mode of action of $Re(CO)_3$ thymidine complexes, ChemMedChem 5 (2010) 1513–1529.
[47] S.E. Aspland, C. Ballatore, R. Castillo, J. Desharnais, T. Eustaquio, P. Goelet, Z. Guo, Q. Li, D. Nelson, C. Sun, A.J. Castellino, M.J. Newman, Kinase-mediated trapping of bi-functional conjugates of paclitaxel or vinblastine with thymidine in cancer cells, Bioorg. Med. Chem. Lett. 16 (2006) 5194–5198.
[48] R.F. Barth, B. Kaur, Rat brain tumor models in experimental neuro-oncology: the C6, 9L, T9, RG2, F98, BT4C, RT-2 and CNS-1 gliomas, J. Neurooncol. 94 (2009) 299–312.
[49] R.F. Barth, D.M. Adams, A.H. Soloway, E.B. Mechetner, F. Alam, A.K.M. Anisuzzaman, Determination of boron in tissues and cells using direct-current plasma atomic emission spectroscopy, Anal. Chem. 63 (1991) 890–893.